

Integrated demand-side management and timetabling for an urban transit system: A Benders decomposition approach

Lixing Yang,^{a,*}, Yahan Lu,^{a,b*} Jiateng Yin,^a Sh. Sharif Azadeh^b

^a School of Systems Science, Beijing Jiaotong University, Beijing, 100044, China; ^b Department of Transport & Planning, Delft University of Technology, Netherlands

The intelligent upgrading of metropolitan rail transit systems has made it feasible to implement demand-side management policies that integrate multiple operational strategies in practical operations. However, the tight interdependence between supply and demand necessitates a coordinated approach combining demand-side management policies and supply-side resource allocations to enhance the urban rail transit ecosystem. In this study, we propose a mathematical and computational framework that optimizes train timetables, passenger flow control strategies, and trip-shifting plans through the pricing policy. Our framework incorporates an emerging trip-booking approach that transforms waiting at the stations into waiting at home, thereby mitigating station overcrowding. Additionally, it ensures service fairness by maintaining an equitable likelihood of delays across different stations. We formulate the problem as an integer linear programming model, aiming to minimize passengers' waiting time and government subsidies required to offset revenue losses from fare discounts used to encourage trip shifting. To improve the computational efficiency, we develop a Benders decomposition-based algorithm within the branch-and-cut method, which decomposes the model into train timetabling with partial passenger assignment and passenger flow control subproblems. We propose valid inequalities based on our model's properties to strengthen the linear relaxation bounds at each node. Computational results from proof-of-concept and real-world case studies on the Beijing metro show that our solution method outperforms commercial solvers in terms of computational efficiency. We can obtain high-quality solutions, including optimal ones, at the root node with reduced branching requirements thanks to our novel decomposition framework and valid inequalities. Our integrated optimization approach reduces the fleet size for operators by at least 8.33% and decreases the waiting time of passengers, thereby validating the effectiveness of our proposed methods.

Key words: Urban rail transit; Train scheduling; Trip booking; Trip shifting; Demand-side management; Benders decomposition

1. Introduction

According to the United Nations (2019), there will be 9.7 billion people worldwide by the year 2050, and it is anticipated that about 70% of the world's population by 2050—up from 55% in 2019—will reside in metropolitan regions. This tendency causes the features of passengers in urban rail transit (URT) systems to change over time, such as their quantitative composition and spatial-temporal distributional characteristics. Take the Beijing rail transit system as an example, it transported

210 million people in 2012 while more than 4.53 billion in 2019. In this context, congestion within URT systems in metropolitan areas has become the norm in operations. *Congestion* refers to the phenomena caused by high density of passengers on platforms and trains. In addition to making passengers uncomfortable and thereby lowering their satisfaction, congestion can cause delays, disruptions, and disturbances.

Congestion is caused by the mismatch between continuously evolving passenger demand and the relatively stable capacity of the URT system. To address this challenge, URT authorities and operators may consider several strategies. Initially, they could invest in technical and social strategies that involve infrastructure and operational improvements, such as expanding the number of lines and adjusting train timetables to increase train frequency (Wang et al. 2023). For example, despite the headway on Beijing Metro Line 10 being reduced to one minute and 45 seconds during the morning peak hour, there were still many standing passengers inside trains (Ministry of Transport of the People’s Republic of China 2022). This highlights the necessity for *demand-side management methods*.

From the demand perspective, one approach is the implementation of a *passenger flow control strategy*, which controls the boarding rate at each station to maintain spare capacity for downstream stations, thereby optimizing capacity utilization. For instance, in 2019, the Beijing metro regularly applied this strategy at 91 stations on weekdays. Another approach is *congestion pricing*, which differentiates peak and off-peak fares. This strategy has been effectively applied in several locations, such as London’s congestion charging for road traffic since 1999 (Transport for London 2024), Singapore’s electronic road pricing in busy areas (Motoring 2024), and the Netherlands where off-peak railway discounts are offered (Nederlandse Spoorwegen 2024). Congestion pricing essentially aims to achieve *trip shifting*, encouraging passengers who intend to travel during peak periods to shift to less congested times, thereby balancing the demand across time periods. The effectiveness of managing congestion through this strategy has been demonstrated in Bao et al. (2023). Thereafter, we define *passenger directing* as the combination of the passenger flow control strategy to limit boarding rates and a pricing strategy that incentivizes passengers to shift their travel times. A more moderate and emerging alternative within URT systems is the *trip booking* strategy, which allows a limited number of passengers to reserve a travel slot a day in advance, bypassing queues outside the station for a passenger flow-controlled entry permit. This reservation system, as explored in our study, enables passengers to reserve a time slot that guarantees platform access and immediate train boarding, rather than requiring them to book specific seats. The Beijing metro applied this strategy in 2020, and by 2021, it reportedly saved passengers a cumulative 40,000 hours in waiting times, with a 88 percent approval rate from users (China News 2020). Given the fundamental supply-demand mismatch driving congestion, integrating these operational

and demand-side strategies presents a more effective approach to managing URT operations amid growing congestion worldwide, which is the focus of this paper.

However, to our knowledge, the development of passenger flow control and trip booking strategies in practical operations currently stands apart from the production of train timetables and relies entirely on operators' manual experience. In particular, the trip-booking strategy, enabled by advancements in intelligent URT systems, is an emerging method still in the proof-of-concept phase in real-world applications. This stage calls for innovative approaches to realize its potential benefits (Xia et al. 2024). Moreover, these demand-side management approaches are mostly managed on a station-by-station basis, which limits the potential for achieving line-wide connectivity (Meng et al. 2022).

While existing research has developed mathematical models and solution algorithms for both the passenger flow control problem and the joint optimization of train timetabling and passenger flow control problem, the integration of train timetabling, passenger directing, and trip booking problem is hardly addressed in the literature. However, experimental results from related studies (e.g., Shi et al. 2018, Lu et al. 2023) consistently indicate that although the number of detained passengers decreases with the implementation of the timetabling and passenger flow control policies compared to scenarios without them, the phenomenon of oversaturation remains. These findings highlight the necessity to collaboratively optimize additional demand-side management methods. Moreover, the algorithms proposed for the joint optimization models mainly focus on the solution efficiency, falling short of finding the exact solutions required in operational planning.

In this paper, we aim to close these gaps by developing an integrated demand-side management and timetabling approach with an exact solution method. Our framework is grounded on three key layers: government, metro corporations, and passengers. The goal is to provide proof-of-concept insights to operators and governments through optimal solutions obtained by the exact solution method. We don't consider game theory approaches or bi-level frameworks with passenger behaviors, as they often lead to models that are challenging to solve exactly within an acceptable timeframe. We also omit the sequential solution approach because it lacks feedback between decisions and often leads to suboptimal solutions. By optimizing timetables, passenger flow control strategies, and providing discounts on ticket prices to encourage passengers to shift trips, the metro corporation maximizes its passenger-oriented resource allocation. Passengers, by shifting their travel plans and making reservations, minimize waiting times. Meanwhile, the government makes up for the metro company's loss of fare revenue by providing additional subsidies.

Specifically, this paper formally addresses *the integrated optimization of trip booking, passenger directing, and train timetabling* (BDTT) problem, incorporating time-dependent passenger demand and a time-varying reservation slot allocation plan. We formulate the BDTT problem as an integer

programming (ILP) model that captures the interdependencies among train timetables, passengers with reserved trips, passengers without reservations, and passengers' trip-shifting plans. The objective is to minimize the weighted sum of passengers' waiting time and governments' additional subsidies provided to incentivize trip shifting. Service fairness among passengers in terms of the possibility of boarding the first train, both with and without reservations, and across different stations is modeled as constraints. To effectively solve the proposed BDTT problem, we introduce a novel decomposition framework for our problem. Our approach is based on Benders decomposition which decomposes the model into a timetabling subproblem combined with partial passenger allocations and a passenger flow control subproblem. We validate our proposed formulation and solution methodology through proof-of-concept and real-world case studies.

The remainder of this paper is organized as follows: Section 2 provides an overview of relevant literature. Thereafter, Section 3 presents a detailed description of the studied problem. In Section 4, we formulate the problem as an integer programming model. In Section 5, we propose the linearization procedure, the tailored decomposition approach and an exact solution method. Section 6 presents numerical results and managerial insights. Lastly, we conclude in Section 7.

2. Literature review

In this section, we give an overview on related research. In Section 2.1, we delve into the collaborative optimization of train timetabling and passenger flow control. Section 2.2 describes how the trip reservation and pricing policies are optimized to improve the matching of supply and demand in existing literature. In Section 2.3, we compare our method with the reviewed state-of-art methods.

2.1. Train timetabling problem combined with passenger flow control

With the surge in passenger demand in recent years, the train timetabling problem combined with passenger flow control has become a hot research topic. A common objective is to minimize passengers' waiting time (Li et al. 2017, Liang et al. 2023, Hu et al. 2023, Yuan et al. 2023).

One of the first related models considering the time-dependent passenger demand has been introduced by Shi et al. (2018). The authors formulated an ILP model to determine the train timetable and the time-dependent passenger flow control strategy, which is solved by a hybrid algorithm combining the local search procedure with CPLEX. Further, Liu et al. (2020) proposed a mixed-integer nonlinear programming (MINLP) model for this problem and designed a Lagrangian relaxation-based solution method. Considering uncertain passenger demand, Lu et al. (2022) formulated a two-stage distributionally robust optimization model where the probability of stochastic scenarios is partially known in advance. Lu et al. (2023) formulated three ILP models for this problem, aiming to generate a reliable train timetable and the train-based passenger flow control strategy to cope with the demand uncertainty in reality. The proposed models based on the Light

Robustness technique can be solved directly by GUROBI, while the scenario-based stochastic programming model is also addressed by the hybrid algorithm. In summary, due to the complexity of models that consider supply-demand coupling relations, most of these studies develop heuristic algorithms to solve the proposed models for the integrated optimization problem of timetabling and passenger flow control.

2.2. Trip reservation and congestion pricing

Trip reservation is a demand management strategy frequently studied in the field of airline marketing and road transportation. In the air transportation area, it usually requires all passengers to buy tickets in advance and thus automatically make reservations (Copeland and McKenney 1988, Rothstein 1985, Barz and Gartner 2016). In contrast, there are a limited number of reservations in the URT system that will not allow all demand to be met, where the allocation plan should be dynamic to match the time-varying characteristics of the passenger demand. For a comprehensive review in the latter area, we recommend Yang and Bell (1998). Liu et al. (2015) has demonstrated that the traffic congestion can be effectively relieved by accommodating reservation requests to the level that the highway capacity allows. More recently, Li et al. (2023) proposed a novel hybrid framework integrating booking and rationing strategies on road traffic, which is formulated as a linear program to maintain the fairness, efficiency, and flexibility of individual choices. The computational results indicate that with the system-optimal integrated scheme of booking and rationing, the relative travel time reduction of each OD pair can be more than 20%. The above two efforts have shown that trip reservations and the integration of booking and rationing are highly promising measures to relieve congestion.

Another demand management measure is congestion pricing, typically by increasing prices during peak hours to reduce demand (i.e., surge pricing) or by decreasing prices in other periods to encourage passengers to shift their departure times (Yang and Wang 2011, Xiao et al. 2015, He et al. 2017, Ding et al. 2023). For example, Robenek et al. (2018) formulated an integrated optimization model for the elastic passenger-centric train timetabling and the pricing problem, which can be solved by a simulated annealing heuristic algorithm. Recently, Yang et al. (2020) proposed a rewards program combined with surge pricing, where riders pay an additional amount to a rewards account during peak periods and then use the balance in the rewards account to subsidize off-peak trips. This paper finds that in some cases, all three stakeholders - i.e., passengers, drivers, and platforms - fare better under this reward scheme combined with surge pricing.

To sum up, the above literature specifically studied the trip booking and congestion pricing problem with the goal of alleviating congestion. The key idea of these two policies is to encourage passengers to shift their travel times, thereby improving the alignment of supply and demand, which is consistent with URT system operations. However, the aforementioned studies mainly focus on road traffic rather than train timetabling and are limited to a single congested bottleneck.

Table 1 Overview of included aspects in the discussed literature. Abbreviations: **HY** = Hybrid method combing heuristic and a standard solver; **SA** = Simulated Annealing; **MA** = Mathematical Analyses; **HE** = Heuristic; **BD**= Benders-decomposition based solution approach.

Publications	Transportation systems	Train timetabling	Passenger directing		Trip reservation	Solution methods
			Passenger flow control	Trip shifting		
Shi et al. (2018)	URT	✓	Time-based			HY
Robenek et al. (2018)	Railway	✓				SA
Yang et al. (2020)	On-demand				✓	MA
Binder et al. (2021)	Railway	✓				SA
Polinder et al. (2022)	Railway	✓				HE
Leutwiler and Corman (2022)	Railway	✓				BD
Bao et al. (2023)	Road			✓		MA
Li et al. (2023)	Road				Static	MA
Leutwiler and Corman (2023)	Railway	✓				BD
Lu et al. (2023)	URT	✓	Train-based			HY
This paper	URT	✓	Train-based		✓	Time-varying BD

2.3. Paper contributions

A wide range of mathematical models and solution methodologies have been explored to develop time-dependent passenger flow control strategies and corresponding train timetables in URT systems, as well as congestion pricing methods aimed at encouraging trip shifting in road traffic. However, most of these approaches are limited to addressing train timetabling, passenger flow control, congestion pricing (or trip shifting), and trip booking problems either separately or with only partial integration. Moreover, they typically rely on heuristic methods to solve the proposed models. While these methods have provided valuable insights, they fall short in guaranteeing solution quality and do not achieve an integrated optimization across potential operational methods, which is essential for maximizing operational efficiency and effectiveness. Table 1 outlines the characteristics of closely related literature, highlighting the contributions of our study, which are detailed as follows.

(1) We formalize the integrated optimization problem of trip booking, passenger directing, and timetabling in the urban rail transit field. Thereafter, we formulate a mathematical model that optimizes train timetables, train-based passenger flow control strategies that are more practically implementable, and passengers’ trip-shifting plans. This model incorporates a time-varying reservation slot allocation plan, ensures service fairness, and adheres to strict capacity limits.

(2) We design a tailored decomposition framework in accordance with the mathematical properties of the proposed model and a Benders-decomposition-based solution method within the branch-and-cut method. In the developed decomposition approach, partial information about passenger dynamics is incorporated into the timetabling subproblem, which can greatly reduce the number of feasibility cuts. Additionally, we introduce valid equalities and inequalities that not only strengthen the bounds at each node but also decrease the number of iterations producing inefficient feasibility cuts. These enhancements enable the proposed algorithm to solve real-world instances within reasonable computational times. We also implement a series of heuristic acceleration strategies to improve the solution quality at the root node.

(3) We validate the methodologies using two series of case studies that consider a proof-of-concept line and the Beijing metro Batong line. The numerical results show the benefits of the proposed approaches from operational efficiency, service fairness, fleet size, and the maximum congestion along the line. The results highlight that the BDDT approach reduces the fleet sizing required to satisfy all passenger demand for operators, and decreases passengers' waiting time compared with only implementing the passenger flow control strategy. Besides, a 23.78% reduction in passenger waiting times is achieved at the expense of a 1.00% increase in government subsidies. Regarding the algorithm, our proposed customized decomposition approach and exact solution method can generate high-quality solutions at the root node, even optimal solutions. In real-world case studies, our algorithm outperforms GUROBI in terms of computing effectiveness.

3. Problem description

In this section, we give a formal description of the BDDT problem for urban rail transit systems. Then, we introduce the assumptions adopted in our model. A framework of practical applications is provided in Figure 12 in Appendix A. In this section, we delve into a more detailed discussion.

3.1. Line structure and time discretization

Consider an oversaturated URT line where passengers arrive during peak periods and frequently experience congestion. The congestion results in them being detained. The set of stations along this line is represented as $\mathcal{S} = \{1, 2, \dots, |\mathcal{S}|\}$, with each station indexed u or v . The section that connects stations u and $u + 1$ is referred to as section u . The set of trains is denoted as $\mathcal{I} = \{1, 2, \dots, |\mathcal{I}|\}$, where train i should depart from the first station and terminate at station $|\mathcal{S}|$. The capacity of each train is denoted by C^{max} . To model the dynamic evolution of trains, the continuous time horizon is discretized into timestamps of duration σ . The set $\tilde{\mathcal{T}} = \{\tilde{t} | 1, 2, \dots, |\tilde{\mathcal{T}}|\}$ corresponds to these discretized timestamps.

3.2. Time-dependent passenger demand and time equalization

Given the aforementioned notations, the time-dependent Origin-Destination (OD) demand for those arriving at station u at timestamp \tilde{t} and heading to station v is denoted as $D_{uv\tilde{t}}$, and the predetermined reservations for the OD pair from stations u to v at timestamp \tilde{t} is denoted as $\hat{D}_{uv\tilde{t}}$. Note that this problem encompasses four indexes: time, trains, the origin and the destination of each passenger. To effectively reduce the dimensionality and to scale down the complexity of the problem, we skew the time dimension at the second station and all subsequent stations. Under this skewed time dimension, the departure time of the train from any station is aligned with its departure from the first station. We define the skewed time as *equivalent time* and denote the studied equivalent time horizon as $\mathcal{T} = \{t | 1, 2, \dots, |\mathcal{T}|\}$, where t is the index of the *discretized*

equivalent timestamp. As for portraying time-dependent passenger demand, its arrival time \tilde{t} is mapped to the corresponding equivalent timestamp t through this skewing operation of the time dimension. Besides, the subset of equivalent timestamps during peak hours is denoted as $\hat{\mathcal{T}}$, which is included within \mathcal{T} , i.e., $\hat{\mathcal{T}} \subseteq \mathcal{T}$.

EXAMPLE 1. *To facilitate understanding of the concept of equivalent time, Figure 1 visually depicts the time coordinate skewing operation. Consider a URT line involving four stations along a line, with two trains operating from stations A to D. The first train originally departs from each station at timestamps 1, 3, 5, and 7, respectively. After applying the proposed skewing operation of the time dimension, the departure times of the first train at all stations are skewed to the first equivalent timestamp. Likewise, the second train leaves each station at the third equivalent timestamp.*

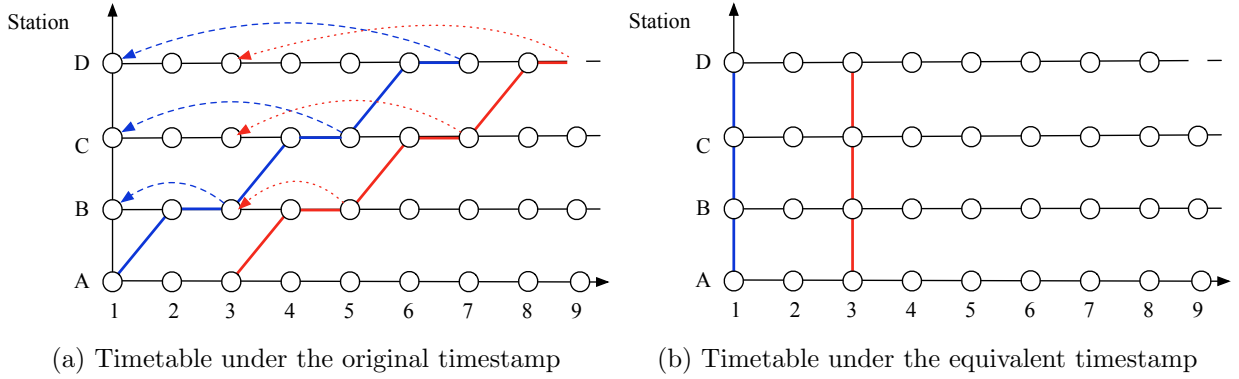


Figure 1 Illustration of timetables under original and equivalent timestamp.

3.3. Categorization of passengers and demand-side management strategies

With advancements in emerging technologies, operators can now utilize intelligent trip reservation systems to implement demand-side management strategies, as adopted by the Beijing metro. These strategies include trip reservations, incentives to encourage off-peak travel, and passenger flow control. Based on these demand-side management methods, passengers can be categorized into three groups: those with reservations, those who attempt to make reservations but are unsuccessful due to limited availability and follow the system's recommended travel times, and those who arrive freely according to their own schedules. The travel time, boarding priority, and fare characteristics for these three passenger types are summarized in Figure 2. Next, we introduce these three types of passengers and the implemented demand-side management strategies in detail.

(i) Passengers with reservations. Let $\hat{D}_{uv,t}$ denote the number of reserved passengers arriving at station u and traveling to station v at time t . These passengers successfully secure reservations for their preferred travel times, granting them the boarding priority. They arrive at their origins

at scheduled times, enter to the platform through dedicated reservation gates, and board the first available train. By paying the full ticket fare, they enjoy seamless boarding upon arrival. Passengers with reservations are not subject to passenger flow control measures and are never stranded.

(ii) Passengers accepting the system’s recommended time. For users of the intelligent reservation system who attempt to make a reservation but cannot secure a slot due to availability limitations, the system offers a suggested arrival time. If the passenger agrees to travel at this recommended time, they receive an incentive. Upon arrival at stations, these passengers are required to queue outside the platform and wait for permission to enter and board a train. In this paper, we consider fare discounts (denoted as ϕ) as the incentive, though other benefits such as credits or cashback could also be offered. By adjusting their scheduled travel time, these passengers gain financial savings and potentially a more comfortable journey with fewer in-vehicle passengers. We define the decision variable $\kappa_{uv}t'$ to represent the number of passengers traveling from station u to station v who shift their arrival time from t to t' . This variable will be determined in the optimization model from a systematic perspective.

(iii) Passengers who arrive freely. These passengers do not use the reservation system or follow its recommendations, arriving instead at their originally planned travel time. Upon arrival, they must queue outside the platform and wait for permission to enter and board trains according to the passenger flow control plan. Unlike passengers who accept the system’s recommended time, freely arriving passengers do not receive any incentives. The passenger flow control plan specifies the number of passengers who are allowed to enter the platform to board the train when a train arrives at a station. This allocation includes both passengers who accept the recommended time and those who arrive freely. We denote the passenger flow control decision variable as b_{iuv} , representing the number of passengers traveling to station v who are permitted to enter the platform to board the train when train i arrives at station u .

REMARK 1. In this paper, we propose a reservation system that does not require passengers to book specific seats, but rather allows them to secure entry to platforms and immediately board trains by reserving a time slot. Seat booking is a common demand management strategy in high-speed rail systems with the large headway, such as China’s and Europe’s (e.g., Germany’s ICE trains and the Eurostar from London to Paris). However, due to the limited seating and high passenger volume during peak hours, metro systems often accommodate standing passengers. For instance, during morning rush hours, the Beijing metro system has more standing than seated passengers. Moreover, in congested metro networks (like the Beijing metro), the headway during peak hours can be as short as 90 seconds. Therefore, it is practical for passengers to simply reserve a time slot, ensuring they can board immediately without the risk of delays and only wait for a maximum of one headway on the platform. In addition, it is worth mentioning that platforms will not be

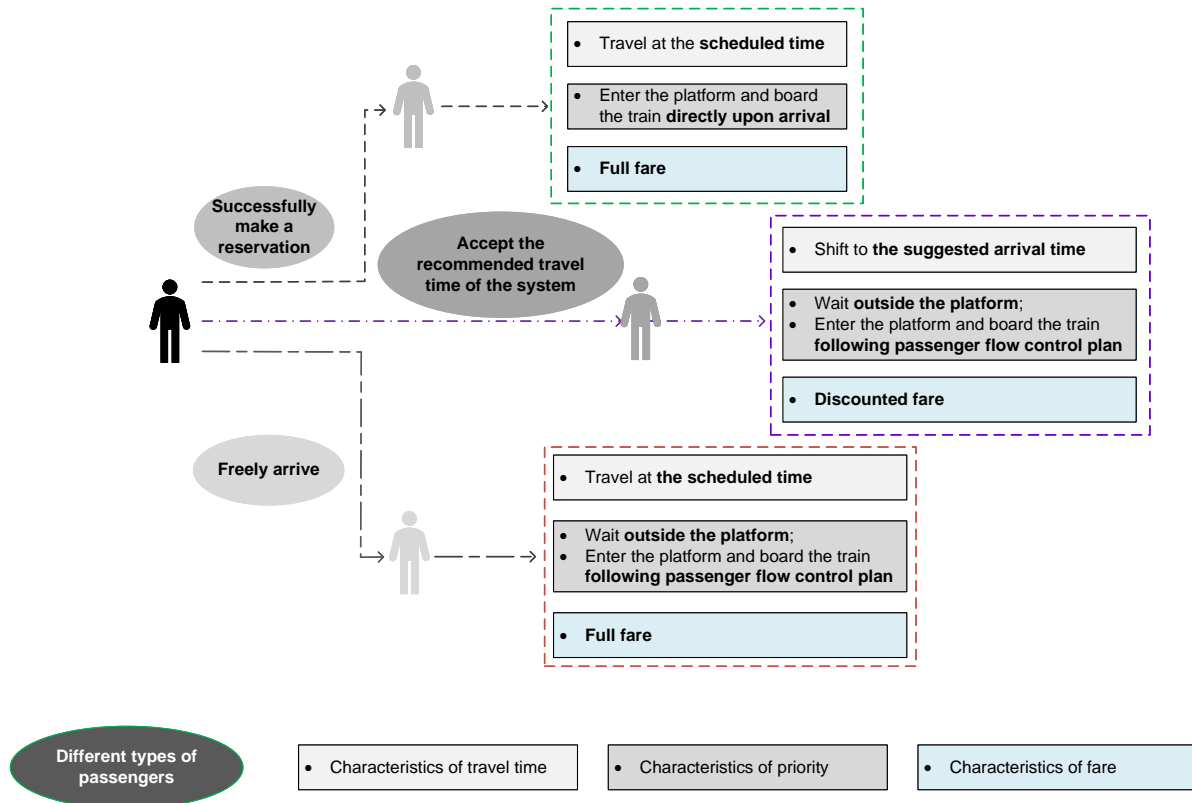


Figure 2 Illustration of passengers' types, travel time, priority, and fare characteristics.

Notes: Passengers with reservations are never detained.

congested, as only passengers with reservations can wait on the platform, and their number is not excessively high.

To further optimize the alignment between supply and demand during peak periods, train timetables are adjusted dynamically in response to time-dependent passenger demand. The timetabling decision variables are denoted as z_{it} , indicating whether train i departs at time t . In summary, we consider the interactions among three key stakeholders: the government, transit operators, and passengers. Figure 3 illustrates these interactions. In a megacity with an overcrowded metro system, the government provides subsidies to the metro corporation to encourage pricing policies that distribute passenger demand more evenly over time. The government aims to minimize these subsidies. Meanwhile, operators focus on optimizing operational strategies from both supply and demand perspectives to improve resource utilization and reduce passenger waiting times. Demand-side management strategies include the pricing method that incentivize trip shifting, a trip-booking approach, and the passenger flow control. Although pricing incentives may reduce revenue, this shortfall is offset by government subsidies. The dynamics of train movements and

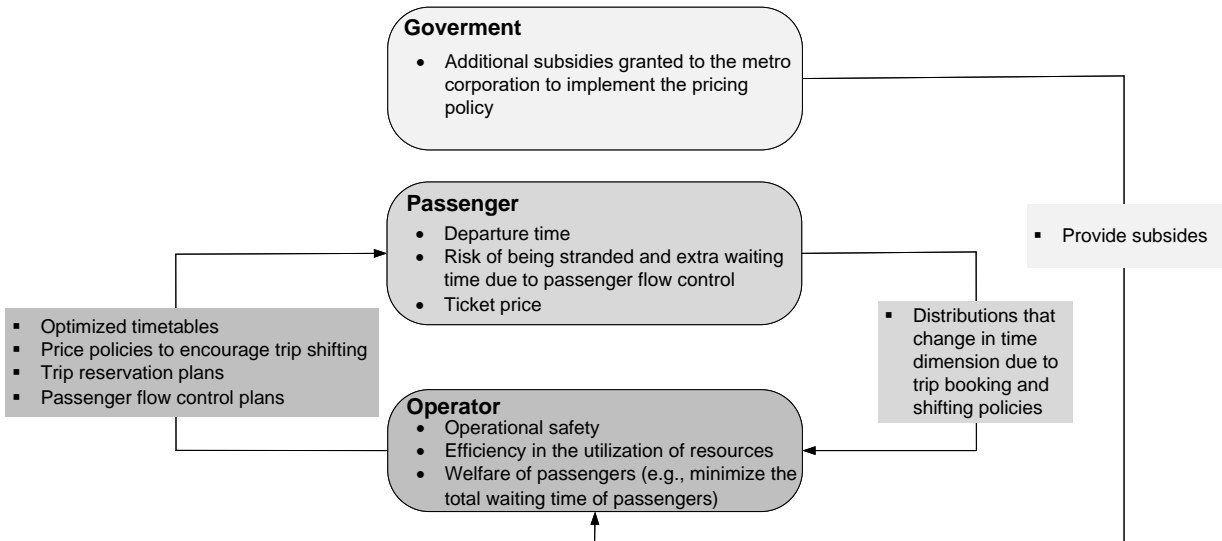


Figure 3 Interactions among the government, passengers, and the operator.

passenger distribution are closely interlinked, with timetables being optimized based on passenger flows. Throughout this paper, we assume that the objective is to minimize a combination of total passenger waiting time and government subsidies. Additionally, we use the terms “additional subsidies” and “lost revenue” interchangeably.

In addition, we make the following assumptions to rigorously formulate the models for the investigated problem.

(i) We assume that information about reservation slots is released to the public through the mobile application. The number of reservations is limited, which can be obtained on a first-come, first-served principle. (The Beijing metro has implemented this application and this demand-side management policy.)

(ii) We focus on weekday scenarios, as commuting behavior is generally more predictable on these days. Thus, we assume that passengers without a reservation can empirically anticipate the level of congestion they would face and the risk of being stranded if they do not shift their arrival times.

(iii) We assume that all reservation slots are selected daily and that reserved passengers are guaranteed to show up on time. Observations from the Beijing metro’s trip reservation show that most reserved passengers are commuters during peak hours, and reservation slots are quickly filled within minutes of release.

(iv) Passenger demand is assumed to be homogeneous and individual behavior is outside the scope of our study. We aim to introduce a proof-of-concept methodology that allows operators and governments to evaluate the effectiveness of integrating demand management strategies with timetabling.

4. Mathematical formulation

In this section, we provide the proposed mathematical model with its associated notations. We then propose two extensions of the proposed model that consider the time-varying pricing strategy and the elastic passenger demand from the other transportation modes.

4.1. INLP model for the BDTT problem

To model the BDTT problem, we introduce three families of decision variables, as listed in Table 2. Specifically, the integer variable $\kappa_{uvt't}$ denotes the number of non-reserved passengers who shift their arrival time at the origin station from t to t' . The second one is the number of non-reserved passengers who are allowed to board train i to reach their destination v , which is denoted as b_{iuv} . The third set of variables z_{it} aims to model the dynamics of trains. The parameters, dependent variables and abbreviations used throughout this paper are summarized in Table 3. We use the following formulation for the BDTT problem, including upper and lower limit constraints on headway, strict capacity constraints, fairness-preserving constraints, and so on.

Table 2 Decision variables in the BDTT model.

Symbol	Definition	Type
$\kappa_{uvt't}$	Number of non-reserved passengers travelling from stations u to v who shift their arrival time from timestamp t to t'	Integer
b_{iuv}	Number of non-reserved passengers heading to station v who are allowed to board train i at station u	Integer
z_{it}	If train i has departed at timestamp t , $z_{it} = 1$; otherwise, $z_{it} = 0$	Binary

Objective function. The objective function (1) minimizes the weighted sum of the passengers' waiting time, and additional government subsidies due to encouraging passengers to shift their departure times, where ω_t and ω_s represent weighting coefficients, respectively. Constraint (2) is formulated to calculate the total waiting time of passengers including both the waiting time and detained time. Constraint (3) computes the additional government subsidies.

$$\min \quad \omega_t F^t + \omega_s F^s \quad (1)$$

$$F^t = \sigma \left[\sum_{i \in \mathcal{I}} \sum_{u \in \mathcal{S}} \sum_{t \in \mathcal{T}} (\hat{p}_{iut}^{wc} + p_{iut}^{wc}) + \sum_{i \in \mathcal{I}} \sum_{u \in \mathcal{S}} \sum_{t \in \mathcal{T}} (x_{it} \sum_{v \in \mathcal{S}_{u+1}} r_{iuv}) \right], \quad (2)$$

$$F^s = \sum_{u \in \mathcal{S}} \sum_{v \in \mathcal{S}_{u+1}} \sum_{t \in \mathcal{T}} \left[D_{uvt} \varepsilon_{uv} - \varepsilon_{uv} \left[\sum_{t+1 \leq t' \leq \min\{|\mathcal{T}|, t+\nu\}} (\phi \kappa_{uvtt'} + \kappa_{uvtt'}) \right] \right]. \quad (3)$$

Waiting time of three types of passengers. Motivated by Xia et al. (2023), constraints (4) - (5) are proposed to compute the number of passengers with and without reservations who newly arrive at station u and timestamp t and wait for train i , and constraints (6) - (7) track the total number of passengers waiting for train i at station u and timestamp t . The binary variable x_{it}

Table 3 Parameters, dependent variables, and abbreviations.

Sets	
\mathcal{I}	Set of trains, $\mathcal{I} = \{1, 2, \dots, \mathcal{I} \}$, indexed by i, j
\mathcal{S}	Set of stations, $\mathcal{S} = \{1, 2, \dots, \mathcal{S} \}$, indexed by u, v, m
\mathcal{S}_{u+1}	Set of stations following station u , $\mathcal{S}_{u+1} = \{u+1, \dots, \mathcal{S} \}$
$\tilde{\mathcal{T}}$	Set of discretized timestamps, $\tilde{\mathcal{T}} = \{1, 2, \dots, \tilde{\mathcal{T}} \}$, indexed by \tilde{t}
\mathcal{T}	Set of discretized equivalent timestamps, $\mathcal{T} = \{1, 2, \dots, \mathcal{T} \}$, indexed by t
$\hat{\mathcal{T}}$	Set of discretized equivalent timestamps during peaking hours, $\hat{\mathcal{T}} \subseteq \mathcal{T}$
Parameters	
σ	Length between two timestamps
s_u	Train running time on the section between stations u and $u+1$
h^{min}	Minimum headway
h^{max}	Maximum headway
C^{max}	Train capacity
ε_{uv}	Ticket price from stations u to v
ϕ	Discount rate of ticket prices
ϱ_{iu}	Service fairness factor of train i at station u
ι	Maximum timestamps that unreserved passengers can shift their travels
D_{uvt}	Number of unreserved passengers who arrive at station u and head to station v at timestamp t
\hat{D}_{uvt}	Number of reserved passengers who arrive at station u and head to station v at timestamp t
ω_t, ω_s	Weighting coefficients
Involved variables	
x_{it}	Binary variable. $x_{it} = 1$ if timestamp t belongs to the headway between train $i-1$ and train i
d_i	Departure time of train i
h_i	Headway between trains $i-1$ and i , defined as the timestamp from the departure time of train $i-1$ to the timestamp just before the departure of train i
$o_{iu}(\hat{o}_{iu})$	Number of on-board passengers without (with) reservations in train i when it departs from station u
$l_{iu}(\hat{l}_{iu})$	Number of passengers alighting from train i without (with) reservations when it arrives at station k
w_{iu}	Number of passengers waiting for train i at station u
w_{iuv}	Number of passengers waiting for train i at station k and head to station v
r_{iuv}	Number of passengers detained by train i at station u and head to station v
\hat{b}_{iuv}	Number of passengers with reservations who are allowed to board train i at station u and head to station v
\hat{p}_{iut}^w	Number of passengers with reservations who arrive at timestamp t and wait for train i at station u
\hat{p}_{iut}^{wc}	Number of non-reserved passengers waiting for train i at station u who arrive at timestamp t
p_{iut}^w	Number of reserved passengers waiting for train i at station u and timestamp t
p_{iut}^{wc}	Number of passengers without reservations who arrive at timestamp t and wait for train i at station u
Abbreviations	
F^t	Total waiting time of passengers
F^s	Total additional government subsidies that arise from incentives to shift trips

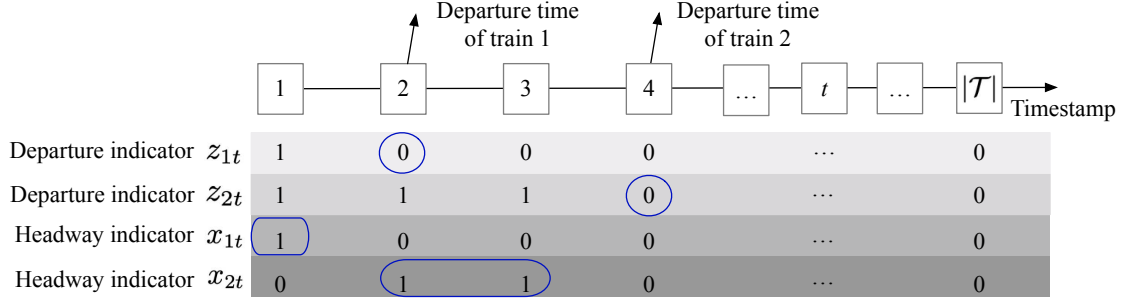


Figure 4 Illustration of departure and headway indicators.

represents the headway indicator, which are coupled with departure indicator z_{it} in the following constraints. Here, the *headway* between trains $i - 1$ and i is defined as the timestamp from the departure time of train $i - 1$ to the timestamp just before the departure of train i . To facilitate understanding, an illustrative example is visualized in Figure 4. It can be seen that two trains depart at the second and fourth timestamps, respectively. Hence, timestamp 1 corresponds to the first headway, while timestamps 2 and 3 belong to the second headway which is between trains 1 and 2.

$$\hat{p}_{iut}^w = x_{it} \sum_{v \in \mathcal{S}_{u+1}} \hat{D}_{uvt} \quad \forall i \in \mathcal{I}, u \in \mathcal{S}, t \in \mathcal{T}, \quad (4)$$

$$p_{iut}^w = x_{it} \sum_{v \in \mathcal{S}_{u+1}} \sum_{t \leq t'' \leq \min\{|\mathcal{T}|, t+i\}} \kappa_{uvtt''} \quad \forall i \in \mathcal{I}, u \in \mathcal{S}, t \in \mathcal{T}, \quad (5)$$

$$\hat{p}_{iut}^{wc} = x_{it} \sum_{t' \in \mathcal{T}, t' \leq t} \hat{p}_{iut'}^w \quad \forall i \in \mathcal{I}, u \in \mathcal{S}, t \in \mathcal{T}, \quad (6)$$

$$p_{iut}^{wc} = x_{it} \sum_{t' \in \mathcal{T}, t' \leq t} p_{iut'}^w \quad \forall i \in \mathcal{I}, u \in \mathcal{S}, t \in \mathcal{T}. \quad (7)$$

Dynamics of trains. Constraints (8) impose restrictions on the binary indicator variables associated with train operations following Lu et al. (2023). Constraints (9) ensure that all trains are operated before the end of the study time horizon. Constraints (10) link the indicator variables and the real-valued departure time of each train. Constraints (11) are formulated to track the headway of any two adjacent trains. Constraints (12) impose the limitations related to headway. Constraints (13) define the binary indicator related to headway, in other words, the time for passengers waiting for train i .

$$z_{i(t+1)} \leq z_{it} \quad \forall i \in \mathcal{I}, t \in \mathcal{T} \setminus \{|\mathcal{T}|\}, \quad (8)$$

$$z_{i|\mathcal{T}|} = 0 \quad \forall i \in \mathcal{I}, \quad (9)$$

$$d_i = \sum_{t \in \mathcal{T} \setminus \{1\}} [t(z_{i(t-1)} - z_{it})] \quad \forall i \in \mathcal{I}, \quad (10)$$

$$h_i = \begin{cases} d_i - \sigma & \text{if } i = 1 \\ d_i - d_{i-1} & \text{if } i \in \mathcal{I} \setminus \{1\} \end{cases}, \quad (11)$$

$$h^{\min} \leq h_i \leq h^{\max} \quad \forall i \in \mathcal{I} \setminus \{1\}, \quad (12)$$

$$x_{it} = \begin{cases} z_{it} & \text{if } i = 1 \\ z_{it} - z_{(i-1)t} & \text{if } i \in \mathcal{I} \setminus \{1\} \end{cases} \quad \forall i \in \mathcal{I}, t \in \mathcal{T}. \quad (13)$$

Interactions between trains and different types of passengers. Due to trip-shifting policies, the distribution of passengers in the time dimension would change. Constraints (14) and (15) ensure that the number of passengers after shifting arrival times remains the same as before.

$$\sum_{\max\{0, t-i\} \leq t' \leq t} \kappa_{uvt't} = D_{uvt} \quad \forall u \in \mathcal{S}, v \in \mathcal{S}_{u+1}, t \in \hat{\mathcal{T}}, \quad (14)$$

$$\kappa_{uvt't} = \begin{cases} D_{uvt} & \text{if } t' = t \\ 0 & \text{otherwise} \end{cases} \quad \forall u \in \mathcal{S}, v \in \mathcal{S}_{u+1}, t \in \mathcal{T} \setminus \hat{\mathcal{T}}. \quad (15)$$

Thereafter, constraints (16) are formulated to ensure passengers with reservations, who are not controlled by the passenger flow control strategies, can board the first coming train.

$$\hat{b}_{iuv} = \sum_{t \in \mathcal{T}} \hat{D}_{uvt} x_{it} \quad \forall u \in \mathcal{S}, v \in \mathcal{S}_{u+1}. \quad (16)$$

Constraints (17) guarantee that all passengers without reservations are served. Constraints (18) are formulated to compute the number of waiting passengers who do not have reservations. Constraints (19) limit the number of boarding passengers, which is not permitted to exceed the number of waiting passengers. In addition, constraints (19) also require that at least ρ_{iuv} percent of passengers without reservations at station u must be served by train i to reach destination v . This set of constraints aims to ensure twofold above-mentioned service fairness. Constraints (20) are formulated to calculate the number of passengers detained by train i at stop u .

$$\sum_{i \in \mathcal{I}} b_{iuv} = \sum_{t \in \mathcal{T}} D_{uvt} \quad \forall u \in \mathcal{S}, v \in \mathcal{S}_{u+1}, \quad (17)$$

$$w_{iuv} = \begin{cases} \sum_{t' \in \mathcal{T}} z_{it'} \sum_{t' \leq t \leq \min\{|\mathcal{T}|, t'+i\}} \kappa_{uvt't} & \text{if } i = 1 \\ \sum_{t' \in \mathcal{T}} z_{it'} \sum_{t' \leq t \leq \min\{|\mathcal{T}|, t'+i\}} \kappa_{uvt't} - \sum_{j=1}^{i-1} b_{juv} & \text{if } i \in \mathcal{I} \setminus \{1\} \end{cases} \quad \forall u \in \mathcal{S}, v \in \mathcal{S}_{u+1}, \quad (18)$$

$$\rho_{iuv} w_{iuv} \leq b_{iuv} \leq w_{iuv} \quad \forall i \in \mathcal{I}, u \in \mathcal{S}, v \in \mathcal{S}_{u+1}, \quad (19)$$

$$r_{iuv} = w_{iuv} - b_{iuv} \quad \forall i \in \mathcal{I}, u \in \mathcal{S}, v \in \mathcal{S}_{u+1}. \quad (20)$$

Lastly, constraints (21) - (24) ensure that the limitation of capacity is met. Constraints (21) compute the number of in-vehicle passengers with reservations when train i leaves station u . Constraints (22) and (23) track these two values with respect to passengers without reservations,

respectively. Constraints (24) models the coupling relations between passengers with and without reservations, which require the total number of in-vehicle passengers cannot exceed the maximum capacity.

$$\hat{o}_{iu} = \sum_{m \leq u, m \in \mathcal{S}} \sum_{v \in \mathcal{S}_{u+1}} \hat{b}_{imv} \quad \forall i \in \mathcal{I}, u \in \mathcal{S}, \quad (21)$$

$$o_{iu} = \begin{cases} \sum_{v \in \mathcal{S}_{u+1}} b_{iuv} & \text{if } u = 1 \\ o_{i(u-1)} - l_{iu} + \sum_{v \in \mathcal{S}_{u+1}} b_{iuv} & \text{if } u \in \mathcal{S} \setminus \{1, |\mathcal{S}|\} \\ 0 & \text{if } u = |\mathcal{S}| \end{cases} \quad \forall i \in \mathcal{I}, \quad (22)$$

$$l_{iu} = \begin{cases} 0 & \text{if } u = 1 \\ \sum_{m=1}^{u-1} b_{imu} & \text{if } u \in \mathcal{S} \setminus \{1\} \end{cases} \quad \forall i \in \mathcal{I}, \quad (23)$$

$$o_{iu} + \hat{o}_{iu} \leq C^{max} \quad \forall i \in \mathcal{I}, u \in \mathcal{S}. \quad (24)$$

Domains of decision variables. Constraints (25) and (26) define variable domains.

$$\mathbf{x}, \mathbf{z} \in \{0, 1\}^{|\mathcal{I}| \times |\mathcal{T}|}, \quad (25)$$

$$\mathbf{d}, \mathbf{h}, \boldsymbol{\kappa}, \mathbf{b}, \mathbf{w}, \mathbf{o}, \mathbf{l}, \hat{\mathbf{b}}, \hat{\mathbf{o}} \in \mathbb{Z}_+. \quad (26)$$

Based on the above discussions, we can now formalize the model as follows

$$\text{minimize} \quad (1) \quad (27a)$$

$$\text{subject to} \quad (2) - (26). \quad (27b)$$

REMARK 2. Two more extensions of the model are formulated, one for congestion pricing and the other incorporates elastic passenger demand from other transportation modes. For the details of these two extensions, we refer to Appendix C.

5. Solution methodology

In this section, we first reformulate the INLP model (27) into a linear version and introduce the model decomposition approach in Section 5.1. In Section 5.2, we detail the Benders cut separation. The accelerating strategies are introduced in Section 5.3. Lastly, the overall framework of our solution method is presented in Section 5.4.

5.1. Model reformulation and decomposition

Our solution approach is based on Benders decomposition (BD) method, which divides the problem into a *relaxed master problem* (RMP) and a *subproblem* (SP). This approach requires access to the model's dual information, which in turn necessitates that both the RMP and SP are linear and that the SP contains only continuous variables. RMP is obtained by projecting out the decision variables

in the SP and contains *Benders cuts*. Benders cuts include the *optimality cuts* and *feasibility cuts*. The solution of RMP provides a lower bound of the optimal value. In the computational process, an iterative solution procedure is designed where the RMP is firstly solved, the information from the RMP is passed to the SP, and then dual information from the SP is obtained to generate Benders cuts. In our implementation, we construct a branch-and-cut tree for the RMP and solve the SP at each node, generating Benders cuts that are subsequently added to the RMP.

Note that our original model (27) contains nonlinear terms in constraints (2), (5), (6), (7), and (18). The original nonlinear model is first linearized to obtain its equivalent integer linear programming (ILP) form since the BD approach needs to use the dual information of the model. Then, the ILP formulation is relaxed where the passenger-related variables are relaxed to be continuous ones. This relaxed model is decomposed into a RMP where the timetabling and assignments of passengers with reservations are determined, and a SP to optimize the passenger flow control decisions. Lastly, the optimal timetable obtained from the relaxed model is fixed and used as input to the ILP model to generate the optimal integer demand-side management solutions.

The linearization process is detailed in Appendix B, which covers each step of converting the nonlinear terms into linear expressions. The full formulation of the ILP model is presented as follows:

$$\begin{aligned} \min \quad & \omega_t F^t + \omega_s F^s \\ \text{s.t.} \quad & (3) - (4), (8) - (16), (19) - (26), (46) - (54). \end{aligned} \tag{28}$$

For the sake of clarity, we now present model (28) as follows:

$$\mathcal{O} = \min\{\Theta|f(\mathbf{z}, \boldsymbol{\kappa}, \mathbf{b}) \geq 0, \mathbf{z} \in \{0, 1\}^{|\mathcal{I}| \times |\mathcal{T}|}, \boldsymbol{\kappa}, \mathbf{b} \in \mathbb{Z}_+\},$$

where we use Θ to represent the objective function that is detailed in (1).

For the purpose of utilizing the BD method, the integer decision variable $\boldsymbol{\kappa}$ and \mathbf{b} in model \mathcal{O} are relaxed as continuous variables, leading to a relaxed problem (denoted as $\tilde{\mathcal{O}}$) in the solution process. Specifically, the resulting model $\tilde{\mathcal{O}}$ can be expressed as follows

$$\tilde{\mathcal{O}} = \min\{\Theta|f(\mathbf{z}, \boldsymbol{\kappa}, \mathbf{b}) \geq 0, \mathbf{z} \in \{0, 1\}^{|\mathcal{I}| \times |\mathcal{T}|}, \boldsymbol{\kappa}, \mathbf{b} \geq 0\}, \tag{29}$$

In the literature, a large body of work employs the aforementioned decomposition method, see Di et al. (2022), Yin et al. (2023). However, by omitting constraints that requires all passengers must be served and the strict limitation on capacity during the timetabling process, the generated timetables may result in infeasibilities. In this case, feasibility cuts are generated and incorporated into the RMP (Benders 1962). To reduce the high number of iterations required to generate relatively weak feasibility cuts, we introduce a novel decomposition approach that incorporates full information

about passengers with reservations and partial information about those without reservations into the RMP. Specifically, model (29) is decomposed into an RMP, which addresses train timetabling and trip-shifting plans, and an SP with fixed timetables to determine passenger flow control plans.

Furthermore, we embed the BD approach into the branch-and-cut framework. At the beginning, we relax the timetabling-related decision variables (i.e., z_{it}) to continuous ones and solve the RMP to the optimum, where no Benders cuts are included. If all the variables z_{it} are integer, we solve the SP and add optimality or feasibility cuts to the RMP. Otherwise, we select a fractional variable z_{it} to run the branch-and-cut process. At each node, we solve the SP and incorporating information from the SP into the RMP. The RMP incorporates only a subset of the Benders cuts, which are added following the procedure proposed in Section 5.2. The RMP and the SP can now be formulated as

$$\min_{\mathbf{z}, \boldsymbol{\kappa}, \theta} \quad \omega_t \sigma \sum_{i \in \mathcal{I}} \sum_{u \in \mathcal{S}} \sum_{t \in \mathcal{T}} (\hat{p}_{iut}^{wc} + p_{iut}^{wc}) + \omega_s F^s + \theta \quad (30a)$$

$$\text{s.t.} \quad \theta \geq \Omega(\mathbf{z}, \boldsymbol{\kappa}) \geq \Omega(\mathbf{z}_l^*, \boldsymbol{\kappa}_l^*) + \boldsymbol{\xi}^T (\mathbf{z} - \mathbf{z}_l^*) + \boldsymbol{\chi}^T (\boldsymbol{\kappa} - \boldsymbol{\kappa}_l^*) \quad \forall l \in \{1, 2, 3, \dots, c_1\}, \quad (30b)$$

$$0 \geq \Omega(\mathbf{z}, \boldsymbol{\kappa}) \geq \Omega(\mathbf{z}_l^*, \boldsymbol{\kappa}_l^*) + \boldsymbol{\xi}^T (\mathbf{z} - \mathbf{z}_l^*) + \boldsymbol{\chi}^T (\boldsymbol{\kappa} - \boldsymbol{\kappa}_l^*) \quad \forall l \in \{1, 2, 3, \dots, c_2\}, \quad (30c)$$

$$\hat{\delta}_{iu} \leq C^{max} \quad \forall i \in \mathcal{I}, u \in \mathcal{S}, \quad (30d)$$

$$(3), (4), (8) - (15), (50) - (52), \quad (30e)$$

$$\mathbf{z} \in [0, 1]^{|I| \times |\mathcal{T}|}, \quad (30f)$$

$$\boldsymbol{\kappa}, \theta \geq 0, \quad (30g)$$

where c_1 and c_2 indicates the number of added optimality and feasibility cuts, respectively. $\Omega(\mathbf{z}, \boldsymbol{\kappa})$ indicates the objective function of SP, and the auxiliary decision variable θ approximates the objective function of SP. For SP, the solution $(\mathbf{z}^*, \boldsymbol{\kappa}^*)$ is fixed. That is,

$$\Omega(\mathbf{z}^*, \boldsymbol{\kappa}^*) = \min_{\mathbf{b}} \left\{ \omega_t \sigma \sum_{i \in \mathcal{I}} \sum_{u \in \mathcal{S}} \sum_{t \in \mathcal{T}} q_{iut} \right\} \quad (31a)$$

$$\text{s.t.} \quad \mathbf{z} = \mathbf{z}^*, \quad (31b)$$

$$\boldsymbol{\kappa} = \boldsymbol{\kappa}^*, \quad (31c)$$

$$\mathbf{b} \geq 0, \quad (31d)$$

$$(13) - (17), (19) - (20), (22) - (24), (46), (53) - (54), \quad (31e)$$

where constraints (31b) and (31c) are the variable-fixing constraints.

5.2. Benders cut separation

As introduced in Section 5.1, we solve the model (29) using a branch-and-cut method and thus dynamically include the Benders cuts while exploring the branch-and-bound tree. At each node in the branch-and-bound tree, optimality or feasibility cuts for the decision variable \mathbf{z} and $\boldsymbol{\kappa}$ is

generated using the dual information of the SP and added into the RMP. In the following, we provide a detailed description of each type of cuts.

First, function $\Omega(\mathbf{z}, \boldsymbol{\kappa})$ can be underestimated by a supporting hyperplane on $(\mathbf{z}^*, \boldsymbol{\kappa}^*)$ because of convexity. If SP (31) given solution $(\mathbf{z}^*, \boldsymbol{\kappa}^*)$ is feasible, the *optimality cuts* are generated as follows:

$$\theta \geq \Omega(\mathbf{z}, \boldsymbol{\kappa}) \geq \Omega(\mathbf{z}^*, \boldsymbol{\kappa}^*) + \boldsymbol{\xi}^T(\mathbf{z} - \mathbf{z}^*) + \boldsymbol{\chi}^T(\boldsymbol{\kappa} - \boldsymbol{\kappa}^*) \quad (32)$$

where $\Omega(\mathbf{z}^*, \boldsymbol{\kappa}^*)$ is the objective value of the SP, $\boldsymbol{\xi}$ and $\boldsymbol{\chi}$ represent the dual variables of constraints (31b) and (31c), respectively.

If SP (31) is infeasible, we feed the following *feasibility cuts* to the RMP

$$0 \geq \Omega(\mathbf{z}, \boldsymbol{\kappa}) := \min\{\mathbf{1}^T \mathbf{s} \mid f(\mathbf{z}, \boldsymbol{\kappa}) \leq \mathbf{s}, \mathbf{s} \geq 0\} \geq \Omega(\mathbf{z}^*, \boldsymbol{\kappa}^*) + \boldsymbol{\xi}^T(\mathbf{z} - \mathbf{z}^*) + \boldsymbol{\chi}^T(\boldsymbol{\kappa} - \boldsymbol{\kappa}^*). \quad (33)$$

To strengthen the optimality cuts (32), Rahmaniani et al. (2020) introduces Benders dual decomposition (BDD) approach which generate the *strengthened optimality cuts*. In the BDD method, the local copies of the variables in the RMP are introduced in the SP and then priced out into the objective function. It was proven that strengthened optimality cuts are tighter than the traditional optimality cuts (32). Specifically, when solving our problem with the BDD approach, the variable-fixing constraints (31b) and (31c) are priced out into the objective function using dual multipliers $\boldsymbol{\xi}$ and $\boldsymbol{\chi}$. By doing so, we obtain the following Lagrangian dual problem

$$\max_{\boldsymbol{\xi}, \boldsymbol{\chi}} \min_{\mathbf{z}, \boldsymbol{\kappa}, \mathbf{b}} \left\{ \omega_t \sigma \sum_{i \in \mathcal{I}} \sum_{u \in \mathcal{S}} \sum_{t \in \mathcal{T}} q_{iut} - \boldsymbol{\xi}^T(\mathbf{z} - \mathbf{z}^*) - \boldsymbol{\chi}^T(\boldsymbol{\kappa} - \boldsymbol{\kappa}^*) : (31d), (31e) \right\}. \quad (34)$$

Then, given $\mathbf{z}^* \in [0, 1]^{|Z| \times |\mathcal{T}|}$, $\boldsymbol{\kappa}^* \in \mathbb{Z}_+$, $\boldsymbol{\xi} \in \mathbb{R}$, and $\boldsymbol{\chi} \in \mathbb{R}$, let $(\hat{\mathbf{z}}^*, \hat{\boldsymbol{\kappa}}^*, \hat{\mathbf{b}}^*)$ be an optimal solution obtained by solving the following problem

$$\min_{\mathbf{z}, \boldsymbol{\kappa}, \mathbf{b}} \left\{ \omega_t \sigma \sum_{i \in \mathcal{I}} \sum_{u \in \mathcal{S}} \sum_{t \in \mathcal{T}} q_{iut} - \boldsymbol{\xi}^{*T}(\mathbf{z} - \mathbf{z}^*) - \boldsymbol{\chi}^{*T}(\boldsymbol{\kappa} - \boldsymbol{\kappa}^*) : (31d), (31e), \mathbf{z} \in [0, 1]^{|Z| \times |\mathcal{T}|}, \boldsymbol{\kappa} \in \mathbb{Z}_+, \mathbf{b} \in \mathbb{R}_+ \right\}. \quad (35)$$

The *strengthened optimality cuts* can be expressed as

$$\theta \geq \Omega(\hat{\mathbf{z}}^*, \hat{\boldsymbol{\kappa}}^*) + \boldsymbol{\xi}^T(\mathbf{z} - \hat{\mathbf{z}}^*) + \boldsymbol{\chi}^T(\boldsymbol{\kappa} - \hat{\boldsymbol{\kappa}}^*). \quad (36)$$

A comparison of the performance of six variants with respect the solution algorithm is presented in the following numerical experiments. The variant based on the BD approach solves the SP at each node and then adds an optimality or feasibility cut to the RMP. On the other hand, in the BDD-based solution method, a strengthened optimality or feasibility cut is generated following the solution of the SP at each node and then integrated into the RMP.

5.3. Strategies for acceleration

In this section, we first introduce two methodologically accelerating methods to strengthen the linear relaxation bounds at each node in Section 5.3.1, subsequently delving into key implementation details which contribute to accelerate computations in Section 5.3.2.

5.3.1. Accelerating methods Firstly, to further guide the timetabling optimization process in the RMP, we propose the following valid equalities and inequalities that incorporate information from non-reserved passengers, which are added into the RMP (30) as constraints.

PROPOSITION 1. *We define the number of passengers without reservations who head to station v and are ensured to board station u as \tilde{b}_{iuv} . Besides, we introduce the number of passengers without reservations who are on board at train i , who depart from train i at station u , and the total number of boarding passengers without reservations at station u as \tilde{o}_{iu} , \tilde{l}_{iu} , and \tilde{b}_{iu} , respectively. For the RMP (30), the following equalities and inequalities are valid:*

$$\tilde{b}_{iuv} = \varrho_{iuv} \sum_{t' \in \mathcal{T}} x_{it'} \sum_{t' \leq t \leq \min\{|\mathcal{T}|, t'+t\}} \kappa_{uvt't} \quad \forall i \in \mathcal{I}, u \in \mathcal{S}, \quad (37)$$

$$\tilde{o}_{iu} = \begin{cases} \sum_{v \in \mathcal{S}_{u+1}} \tilde{b}_{iuv} & \text{if } u = 1 \\ \tilde{o}_{i(u-1)} - \tilde{l}_{iu} + \sum_{v \in \mathcal{S}_{u+1}} \tilde{b}_{iuv} & \text{if } u \in \mathcal{S} \setminus \{1, |\mathcal{S}|\} \\ 0 & \text{if } u = |\mathcal{U}| \end{cases} \quad \forall i \in \mathcal{I}, \quad (38)$$

$$\hat{o}_{iu} + \tilde{o}_{iu} \leq C^{max}, \quad \forall i \in \mathcal{I}, u \in \mathcal{S}, \quad (39)$$

$$\tilde{l}_{iu} = \begin{cases} 0 & \text{if } u = 1 \\ \sum_{m=1}^{u-1} \tilde{b}_{im_u} & \text{if } u \in \mathcal{S} \setminus \{1\} \end{cases} \quad \forall i \in \mathcal{I}, \quad (40)$$

$$\tilde{b}_{iu} = \sum_{v \in \mathcal{S}, v > u} \tilde{b}_{iuv} \quad \forall i \in \mathcal{I}, u \in \mathcal{S}. \quad (41)$$

Proof. Recall that we require at least ϱ percent of passengers without reservations to be served by each train to ensure fairness in the SP (31), that is, constraints (19). Therefore, for any $\mathbf{z} \in [0, 1]^{|\mathcal{I}| \times |\mathcal{T}|}$ generated in the RMP, if this timetable is feasible, then it must serve ϱ (unit: percent) of passengers without reservations while satisfying capacity limitation (24). Being inspired by this property, we integrate the dynamics of ϱ (unit: percent) of passengers without reservations into the RMP. To be specific, the number of passengers without reservations who head to station v and are guaranteed to board train i at station u is formulated as constraints (37). Thereafter, constraints (38) model the number of in-vehicle passengers without reservations. Constraints (39) are formulated to ensure the capacity limitation, which is the key inequalities that enhance the lower bound of the RMP. Hence, Proposition 1 holds. \square

Secondly, it is widely recognized that the effectiveness of the branch-and-bound method is significantly influenced by the *Big-M* values in formulations, which returns poor bounds and causes large branching trees. To enhance solution efficiency, we tighten the upper bounds by redefining the *Big-M* values in constraints (46), (48), (51), and (53). Specifically, considering that the parameter M_u in constraints (46) represents the upper limitation of the detained passengers, its minimum value without cutting out the optimal solution is the one where all the non-reserved passengers are not served during the study time horizon. Thus, we redefine the M_u as follows.

$$M_u = \sum_{t \in \mathcal{T}} \sum_{v \in \mathcal{S}_{u+1}} (1 - \varrho_{uv}) D_{uvt} \quad u \in \mathcal{S}. \quad (42)$$

Similarly, M_{ut} in constraints (48), $M_{ut'}$ in constraints (51), and $M_{uvt'}$ in constraints (53) can be defined as:

$$M_{ut} = \sum_{v \in \mathcal{S}_{u+1}} \sum_{t' \leq t' \leq \min\{|\mathcal{T}|, t+i\}} D_{uvt'} \quad \forall u \in \mathcal{S}, t \in \mathcal{T}. \quad (43)$$

$$M_{ut'} = \sum_{v \in \mathcal{S}_{u+1}} \sum_{t' \leq t'' \leq \min\{|\mathcal{T}|, t'+i\}} D_{uvt''} \quad u \in \mathcal{S}, t' \in \mathcal{T}. \quad (44)$$

$$M_{uvt'} = \sum_{t' \leq t \leq \min\{|\mathcal{T}|, t'+i\}} D_{uvt} \quad \forall u \in \mathcal{S}, v \in \mathcal{S}_{u+1}, t' \in \mathcal{T}. \quad (45)$$

5.3.2. Heuristic accelerating strategy Moreover, we accelerate the solution by incorporating the following ideas from Fischetti et al. (2016) and Fischetti et al. (2017).

Cut loop at the root node. We implement the accelerating method at each cut loop iteration. Specifically, we have two points at the decision variables at each cut loop iteration: the optimal solution $(\mathbf{z}^*, \boldsymbol{\kappa}^*)$ of the current RMP and a stabilizing point $(\tilde{\mathbf{z}}, \tilde{\boldsymbol{\kappa}})$ that is initialized by solving the following problem:

$$\max \left\{ \sum_{i \in \mathcal{I}} \sum_{t \in \mathcal{T}} z_{it} + \sum_{u \in \mathcal{S}} \sum_{v \in \mathcal{S}_{u+1}} \sum_{t \in \mathcal{T}} \sum_{t' \leq t \leq \min\{|\mathcal{T}|, t'+i\}} \kappa_{uvt't} \mid (\mathbf{z}, \boldsymbol{\kappa}) \in \mathcal{X} \right\},$$

where \mathcal{X} is the domain of decision variables $(\mathbf{z}, \boldsymbol{\kappa})$. At each step, we move $(\tilde{\mathbf{z}}, \tilde{\boldsymbol{\kappa}})$ towards $(\mathbf{z}^*, \boldsymbol{\kappa}^*)$ by setting $(\tilde{\mathbf{z}}, \tilde{\boldsymbol{\kappa}}) = (\alpha \tilde{\mathbf{z}} + (1 - \alpha) \mathbf{z}^*, \alpha \tilde{\boldsymbol{\kappa}} + (1 - \alpha) \boldsymbol{\kappa}^*)$ and then apply our optimality cuts to the intermediate point $(\lambda \mathbf{z}^* + (1 - \lambda) \tilde{\mathbf{z}}, \lambda \boldsymbol{\kappa}^* + (1 - \lambda) \tilde{\boldsymbol{\kappa}})$, where parameters $\lambda \in (0, 1]$ and $\alpha \in (0, 1]$. Then, the intermediate point is fed to the SP (31). The optimality cuts (32) are updated and statically added to the RMP. After five consecutive iterations which the linear programming (LP) bound does not improve, parameter λ is reset to one and the cut loop continues.

Tailing off. We prevent more than v successive calls of the Benders cut separation functions (32) and (36) (\hat{v} for the root node) at each fractional node of the branch-and-cut tree. In order to ensure correctness, integer solutions capable of updating the incumbent are always separated.

Restart. Before entering the final branch-and-cut run, we stop the execution right after the root node, add the generated Benders cuts as static cuts to the RMP, update the incumbent, and repeat. This restart mechanism is applied twice before entering the final run in our implementation.

Tree search. We aggressively apply the level of all GUROBI’s internal cuts, select the full-strong branching, and use the strongest lower-bound searching strategies. As to heuristics, we apply the relaxation induced neighborhood search heuristic at every node to feed our Benders-cut separator with low-cost integer solutions.

5.4. Overall framework

With these definitions in place, the decomposition algorithm within branch-and-cut framework can be outlined in Algorithm 1, which can be summarized as follows: (1) At the root node, relax the variable \mathbf{z} and solve the RMP (30) to the optimum. It is worth noting that no optimality cut or feasibility cut has been included. (2) Identify a fractional $z_{i,t} \notin \{0,1\}$ from the solution at the root node and perform branching on this variable to create two new nodes. (3) At each subsequent node within the branch and bound tree, solve the RMP, and feed its solution into the SP (31). Subsequently, an optimality, strengthened optimality, or feasibility cut is added to the RMP, followed by the evaluation to check if the relaxed Gap, defined as $(UB - LB)/LB \times 100\%$, falls below the pre-given tolerance ε_1 . Once this criterion is met, the timetabling solution \mathbf{z}_0^* is input into the ILP model (28), which includes the integer decision variables $\boldsymbol{\kappa}, \mathbf{b}$. GUROBI is employed to solve this model to optimality.

6. Numerical experiments

In this section, two series of numerical experiments are constructed to demonstrate the effectiveness of our proposed approaches. First, in Section 6.1, we evaluate the advantages of the proposed models and the performance at the root node of the solution method on a proof-of-concept case study. Thereafter, to gain more insights on the integrated optimization and the full performance of the algorithm, we conduct real-world instances based on the data of Beijing metro in Section 6.2. The model and the solution method are coded in Java in combination with GUROBI 9.5.1. The experiments are run on a personal computer equipped with an Intel i9-14900HX CPU at 2.20 GHz and 64 GB of RAM.

6.1. Proof-of-concept case study

The proof-of-concept case study involves a metro line with six stations, as shown in Figure 5. It is assumed that the section running times and dwell times at each station are one minute. Furthermore, the minimum and maximum headways are set as two and six minutes, respectively, with each train having a capacity of 600 passengers. For the time horizon, a period of 60 minutes is

Algorithm 1 The Benders decomposition algorithm for the Problem (28)

Require: The set of stations \mathcal{S} , the set of trains \mathcal{I} , the set of timestamps \mathcal{T} , the time-varying OD demand \mathbf{D} , the reservations $\hat{\mathbf{D}}$, the tolerance $0 \leq \varepsilon_1 \leq 100$

- 1: Set the lower bound (LB) as $-\infty$, and set the upper bound (UB) as $+\infty$. Create an empty list of nodes and insert the root node into that list.
- 2: **while** $(UB - LB)/LB \times 100\% > \varepsilon_1$ **do**
- 3: **if** the node list is empty **then**
- 4: **break**
- 5: **else**
- 6: **if** the objective value at the current node is greater than or equal to UB **then**
- 7: Fathom the current node and return to the beginning of the loop;
- 8: **else**
- 9: Select and branch on a non-binary variable. Remove the current node and append the resulting two branch nodes to the list of pending nodes.
- 10: Select a pending node from the node list; Let $(\tilde{\mathbf{z}}, \tilde{\boldsymbol{\kappa}})$ be the solution of the RMP (30) at this node, obtaining the optimal solution. Update LB .
- 11: Solve the SP (31) under the solution $(\tilde{\mathbf{z}}, \tilde{\boldsymbol{\kappa}})$.
- 12: **if** SP is feasible **then**
- 13: Obtain the optimal solution $\tilde{\mathbf{b}}$ of SP.
- 14: Add the optimality cuts (32) or the strengthened optimality cuts (36) to the RMP.
- 15: Calculate $\tilde{UB} = \omega_t F^t(\tilde{\mathbf{z}}, \tilde{\boldsymbol{\kappa}}, \tilde{\mathbf{b}}) + \omega_s F^s(\tilde{\mathbf{z}}, \tilde{\boldsymbol{\kappa}}, \tilde{\mathbf{b}})$.
- 16: **if** $\tilde{UB} < UB$ **then**
- 17: Set $UB = \tilde{UB}$.
- 18: Update $(\mathbf{z}_0^*, \boldsymbol{\kappa}_0^*, \mathbf{b}_0^*)$ to be $(\tilde{\mathbf{z}}, \tilde{\boldsymbol{\kappa}}, \tilde{\mathbf{b}})$.
- 19: **end if**
- 20: **else**
- 21: Add feasibility cuts (33) to the RMP.
- 22: **end if**
- 23: **end if**
- 24: **end if**
- 25: **end while**
- 26: Use \mathbf{z}_0^* to solve Problem (28) using Gurobi, obtaining the optimal integer solution $(\mathbf{z}^*, \boldsymbol{\kappa}^*, \mathbf{b}^*)$.
- 27: **return** $(\mathbf{z}^*, \boldsymbol{\kappa}^*, \mathbf{b}^*)$

considered, which is discretized into one-minute timestamps. Time-varying OD passenger demand is randomly generated to simulate realistic situations from peak-hour to off-peak-hour periods. The fare on each OD pair is set as 3 RMB.

To derive insights into the operational strategies integrating booking, directing and timetabling, sensitivity analyses related to various parameter settings are presented in Section 6.1.1. In Section 6.1.2, a comparison of the lower and upper bounds at the root node among the six variants of the proposed algorithm is conducted to evaluate their effectiveness.

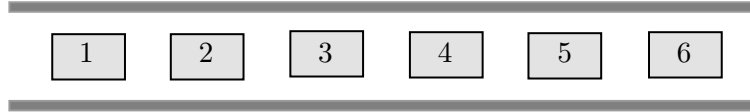


Figure 5 An illustration of the proof-of-concept line.

6.1.1. Managerial insights This section assesses the value of integrating directing and timetabling decisions, and provides insights into the trade-off between operational effectiveness and service fairness as well as the interests of passengers and the operator. To do so, we first fix the service fairness parameters and weight coefficients in the objective function, and analyze the resulting service efficiency and the additional government subsidies among various shifting limitations. Further, we construct a set of experiments by varying the booking ratio. Lastly, we use the concept of ε -Constraints to find Pareto solutions, where it is impossible to reduce the additional government subsidies without increasing the waiting time, and vice versa.

Our managerial insights quantify the benefits of directing and timetabling simultaneously (Insight 1), ensuring service fairness in optimizing passengers' and resources' assignments (Insight 2) and improving operational efficiency through the pricing policy (Insight 3).

INSIGHT 1. Encouraging 21.14% of passengers to shift their arrival times by up to 10 minutes through providing a discount on tickets would result in savings of at least 8.33% in the fleet size and at the expense of a 2.03% reduction in the additional subsidy.

In Table 4, the results among various maximum values of shifting time are presented, where both the booking ratio (i.e., $\hat{D}_{uvt}/(\hat{D}_{uvt} + D_{uvt}) \forall u, v \in \mathcal{S}, v \geq u, t \in \mathcal{T}$) and the service fairness factor ϱ_{iu} for all $i \in \mathcal{I}, u \in \mathcal{S}$ are set to 50%, the discount on the ticket price is 20%, and the weight coefficients are designated as 1 and 5. These results include the percentage of passengers shifting departure times (SP), the average waiting time of passengers without reservations (AWT-WR), the number of detained passengers without reservations (DP), the percentage of additional government subsidies, and the maximum congestion experienced at stations during the operation of all trains. SP and AWT-WR are computed as

$$(\text{Results}/\# \text{ of passenger without reservations}) \times 100 (\%),$$

Table 4 Results among various values of maximum allowable shifting time. Abbreviations: SP= Shifting passengers; AWT-WR = Average waiting time of passengers without reservations; DP = Detained passenger; MW = Maximum number of passengers waiting at stations.

# of trains	Maximum shifting time (min)	SP (%)	AWT-WR (min)	# of DP	Additional subsidy (%)	MW
11	0	Infeasible	—	—	—	—
	5	Infeasible	—	—	—	—
	10	21.14	2.48	211.00	2.03	312.00
	15	26.25	1.91	32.00	2.52	236.00
	20	22.48	1.93	32.00	2.16	225.00
	25	22.75	1.92	32.00	2.19	236.00
12	0	0	2.53	202.00	0	245.00
	5	14.22	1.93	0	1.37	231.00
	10	15.64	1.87	0	1.50	227.00
	15	16.28	1.84	0	1.56	212.00
	20	12.76	1.93	0	1.23	231.00
	25	14.00	1.90	0	1.35	214.00

$(\text{Additional subsidies}/\text{Revenue when shifting is not allowed}) \times 100 (\%)$.

It can be observed that when the demand management strategy encouraging passengers to shift trips through incentives is not implemented, at least 12 trains are required to serve all demand. However, if passengers are encouraged to shift their travel by up to 10 minutes, it becomes possible to meet all demand with just 11 trains. This finding leads us to conclude that a demand management strategy that promotes passenger shifts through incentives can effectively reduce fleet size.

A second observation is there is an inverse relationship between the elasticity in arrival time adjustments and the reduction of the number of detained passengers. Specifically, as passengers' shifting behavior is encouraged and the duration of maximum shifting time extends, the number of detained passengers is remarkably reduced. For example, when 11 trains are operated, the number of detained passengers decreases from 211 to 32 as the maximum shifting time changes from 10 to 25 minutes. However, there is no linear connection between the maximum allowable shifting time and the average waiting time. This is because the optimal solution is a trade-off between the waiting time and additional government subsidies. These results indicate that the integration of directing and timetabling policies could increase the effectiveness of the rail transit system. This improvement is demonstrated by a considerably reduction in the waiting time of passengers without doing any serious harm to the operator's perspective.

INSIGHT 2. Neglecting the principle of service fairness in the allocation of transit resources increases up to 7.51% in the percentage of passengers necessitating a shift in their departure times. Besides, it leads to a rise in the total waiting time, observed as 19.74% while a 1.93% reduction in the additional government subsidies due to the number of passengers with reservations increases, who do not have the flexibility to shift travel times.

In Figure 6, we present the results among various booking ratios, under the operational parameters of 11 trains, the discount of 20%, a service fairness factor of 50%, a maximum allowable shifting time of 15 minutes, and weight coefficients established at 1 and 5. Here, the booking ratio refers to the ratio of booked passengers to all passenger demand. An increase in the total waiting time with higher booking ratios is observed, which can be attributed to the lack of temporal flexibility of passengers with reservations. These passengers, constrained by their booking commitments, are unable to realign their departure times to match the optimized timetable in order to reduce waiting times. This finding is further corroborated by the trends depicted in Figure 6(b), where we observe that the percentage of passengers who have to alter their departure times increase as the booking ratio changes from 10% to 60%. This alteration arises as a consequence of the occupancy of capacity by reserved passengers adhering to their predetermined departure times, thus forcing a shift among those without reservations to accommodate the system's operational constraints. Moreover, the model is infeasible when the booking ratio is set to 70%. This result indicates that when too many bookings are announced for passengers, it not only becomes more unfair to those who do not have reservations, but it also prevents some booked passengers from being able to access platforms directly. To sum up, the aforementioned findings show the complexity of achieving a balance between service fairness and system efficiency, highlighting the necessity for strategic planning in the allocation of reservations within the rail transit framework.

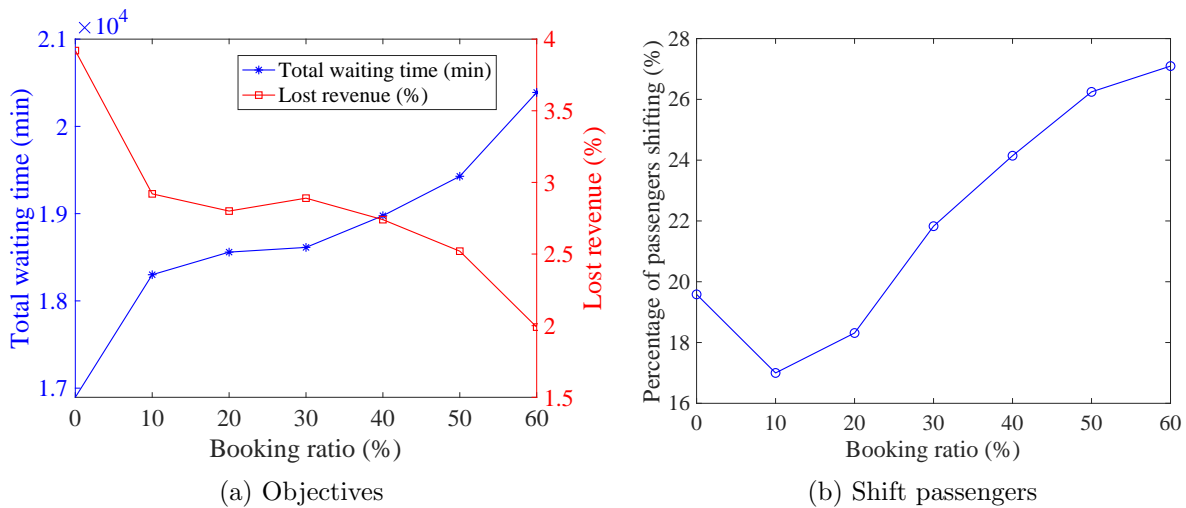


Figure 6 Results among various booking ratios.

INSIGHT 3. Substantial decreases in the waiting time of passengers (23.78%) can be achieved at the cost of very limited increases in the lost revenue of the operator (1.00%).

To further analyze the benefit of integrating timetabling, booking and directing, Figure 7 depicts the decrease in waiting time of passengers and the increase in the additional government subsidies

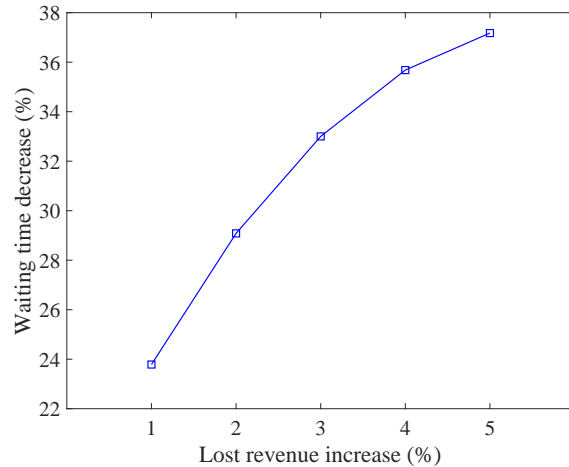


Figure 7 Decrease in waiting time plotted against the increase in the lost revenue, both relative to the solution with the minimum loss of revenue.

for all Pareto solutions, relative to the solution with minimum additional government subsidies. To be specific, the objective function is modified as F^s to generate the solution with minimum loss of revenue (i.e., the additional government subsidies), resulting in a reduction of 0.51% relative to the original revenue computed as $\sum_{u \in \mathcal{S}} \sum_{v \in \mathcal{S}_{u+1}} \sum_{t \in \mathcal{T}} D_{uvt} \varepsilon_{uv}$. Then, the objective function is modified as F^t and a new constraint $F^s \leq \varepsilon$ are added. Here, $\varepsilon = (0.51\% + \xi) \times \sum_{u \in \mathcal{S}} \sum_{v \in \mathcal{S}_{u+1}} \sum_{t \in \mathcal{T}} D_{uvt} \varepsilon_{uv}$, where ξ represents the increment of the allowed lost revenue. Finally, we add the allowed lost revenue with a step size of 1%, and the Pareto optimal points are obtained, as shown in Figure 7.

It turns out that a strategic decision to accept a slight 3% rise in the additional government subsidies can result in a pronounced 33.00% reduction in waiting time. This result indicates the operational efficiency can be enhanced considerably with a relatively minor increase in the additional government subsidies from the operator's perspective. All in all, this is a meaningful observation for transit authorities and operating companies, as they can slightly increase the government subsidies to significantly enhance the people's sense of well-being in traveling through public transportation systems. In the longer term benefit, savings in passengers' waiting time have the potential to translate to higher user satisfaction and increased ridership.

6.1.2. Performance of all variants of solution methods at the root node. To examine the effectiveness of the proposed algorithm, we define the following six variants:

- (i) **BD** uses the optimality and feasibility cuts.
- (ii) **TCBD** extends BD by including the cut loop stabilization at the root node and the tailing off strategy.
- (iii) **TTCBD** extends TCBD by including the tree search strategy.
- (iv) **TTSCBD** extends TTCBD by including the strengthened optimality cuts.

(v) **TRTCBD** extends TTCBD by including the restart strategy.

(vi) **TRTSCBD** extends TTSCBD by including the restart strategy.

Prior to assessing the full performance of the variants, we first examine the impact that the strategies embedded in the solution methods have on the lower and upper bounds at the root node. In this set of experiments, the booking ratio and the serving fairness factor of passengers without reservations are set as 50% and 20%, respectively. Additionally, the discount on the ticket price is set at 20%. The weight coefficients in the objective function are assigned values of 1 and 10, respectively.

Table 5 Lower and upper bounds at the root node for all variants of the solution method.

Instance index (# of trains, # of maximum shifting timestamps, # of timestamps during peak hours)	Root Node	BD	TCBD	TTCBD	TTSCBD	TRTCBD	TRTSCBD
A (12, 5, 35)	Lower Bound	20,492.25	20,424.86	21,408.66	21,809.93	21,414.98	21,829.58
	Upper Bound	–	–	21,847.66	22,225.62	21,847.66	21,847.66
	Root Node Gap (%)	–	–	2.01	1.87	1.98	0.08
B (12, 15, 35)	Lower Bound	19,931.46	19,871.13	21,593.46	21,524.36	21,562.38	21,846.26
	Upper Bound	–	–	21,601.12	21,601.12	21,601.12	21,853.24
	Root Node Gap (%)	–	–	0.03	0.18	0.18	0.03
C (15, 5, 35)	Lower Bound	12,428.30	12,730.73	17,093.40	17,380.99	17,452.86	17,477.00
	Upper Bound	–	–	17,501.00	17,477.00	17,477.00	17,477.00
	Root Node Gap (%)	–	–	2.33	0.55	0.14	0
D (18, 5, 35)	Lower Bound	0	12,056.10	14,573.57	14,805.82	15,056.99	15,028.79
	Upper Bound	11,914.78	18,107.00	15,334.00	15,334.00	15,334.00	15,334.00
	Root Node Gap (%)	100.00	33.42	4.96	3.44	1.81	1.99
E (22, 5, 20)	Lower Bound	13,096.65	13,123.82	13,155.36	13,160.19	13,171.69	13,183.00
	Upper Bound	13,183.00	13,183.00	13,183.00	13,199.00	13,183.00	13,183.00
	Root Node Gap (%)	0.66	0.45	0.21	0.29	0.09	0
F (22, 5, 30)	Lower Bound	13,114.52	13,102.33	13,180.85	13,182.03	13,182.53	13,144.14
	Upper Bound	13,265.00	12,236.00	13,211.00	13,265.00	13,227.00	13,183.00
	Root Node Gap (%)	1.13	1.01	0.23	0.63	0.34	0.29
G (22, 5, 40)	Lower Bound	13,072.24	13,057.69	13,173.06	13,183.00	13,141.95	13,182.37
	Upper Bound	13,265.00	13,550.00	13,265.00	13,198.00	13,218.00	13,198.00
	Root Node Gap (%)	1.45	3.63	0.69	0.11	0.58	0.12

In Table 5, we present the lower and upper bounds at the root node, as well as the *Root node Gap* at the root node among instances characterized by varying numbers of trains, timestamps, and maximum values for shifting timestamps. The Root node Gap represents the relative difference between lower and upper bounds, calculated using the formula

$$\left[\frac{\text{Upper bound} - \text{Lower bound}}{\text{Lower bound}} \right] \times 100 (\%).$$

From the results in Table 5, the following three observations emerge. First, when comparing TRTCBD to BD, there is a substantial decrease in the root node gap. For example, it can be seen that the root node gap decreases from 100% to 1.98%, from 100% to 0.18% at Instances A and B, respectively. Second, on average, the strengthened optimality cuts contribute to tightening both the lower bound and the gap at the root node. In particular, in Instances A, B, C, and E, TRTSCBD

can find the optimal solution at the root node. Lastly, we observe the benefit of incorporating the tree search strategy as it narrows the root node gap in all instances when comparing the TTCBD to TCBD.

6.2. Real-world case study

The instances used for the experiments are derived from the Beijing metro Batong line, which has 13 stations as depicted in Figure 8. This metro line serves as a feeder line, transporting commuters from the suburban district to the city center during morning peak hours. In 2018, nine stations on this line have implemented routine passenger flow control strategies in weekdays to cope with high volume of passenger demand. Tables 6 and 7 provide detailed information about running times on sections, the dwell time at each station, and the distance-based ticket prices used in practice, respectively. On this basis, we consider five instances with varying study time horizons, as detailed in Table 8. To construct these instances, continuous time periods are discretized into one-minute timestamps. The maximum and minimum headways are set to 360 and 120 seconds, respectively. The maximum number of passengers that a train can accommodate is 2,000. In addition, a discount of 20% is offered to passengers who are willing to shift their travel times.

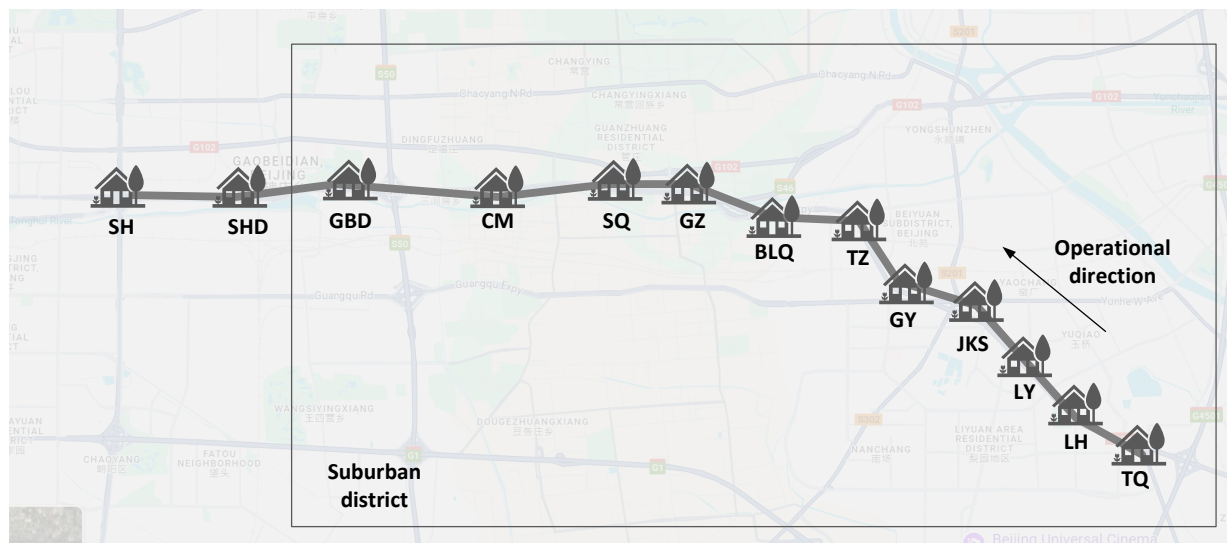


Figure 8 An illustration of the Beijing metro Batong line (Source: Google map).

6.2.1. Performance comparison between different solution methods We first evaluate the full performance of the algorithms. In Table 9, we present the objective function values (abbreviated as Obj.) and the computational times (abbreviated as Time) obtained by GUROBI and six variants of solution methods within a Gap limit of 5%. It can be seen that the cut loop, tailing off, and tree search strategies are able to reduce the computational time considerably. For

Table 6 Dwell and running times on the Beijing metro Batong line.

Station index	Station name (Abbreviation)	Dwell time (in: second)	Section	Running time (in: second)
1	Tuqiao (TQ)	60	Tuqiao→ Linheli	120
2	Linheli (LHL)	60	Linheli → Liyuan	120
3	Liyuan (LY)	60	Liyuan → Jiukeshu	120
4	Jiukeshu (JKS)	60	Jiukeshu→ Guoyuan	120
5	Guoyuan (GY)	60	Guoyuan→ Tongzhou	120
6	Tongzhou (TZ)	60	Tongzhou→ Baliqiao	180
7	Baliqiao (BLQ)	60	Baliqiao→ Guanzhuang	180
8	Guanzhuang (GZ)	60	Guanzhuang→ Shuangqiao	180
9	Shuangqiao (SQ)	60	Shuangqiao→ Chuanmei Uni	180
10	Chuanmei Uni (CM)	60	Chuanmei Uni→ Gaobeidian	180
11	Gaobeidian (GBD)	60	Gaobeidian→ Sihui East	120
12	Sihui East (SHE)	60	Sihui East→ Sihui	180
13	Sihui (SH)	60		

Table 7 The distance-based ticket price of Beijing metro Batong Line (unit: RMB)

Station	1	2	3	4	5	6	7	8	9	10	11	12	13
1	0	3	3	3	3	3	4	4	4	4	5	5	5
2	0	0	3	3	3	3	4	4	4	4	5	5	5
3	0	0	0	3	3	3	3	4	4	4	5	5	5
4	0	0	0	0	3	3	3	3	4	4	4	5	5
5	0	0	0	0	0	3	3	3	3	4	4	5	5
6	0	0	0	0	0	0	3	3	3	4	4	4	5
7	0	0	0	0	0	0	0	3	3	3	4	4	4
8	0	0	0	0	0	0	0	0	3	3	3	4	4
9	0	0	0	0	0	0	0	0	0	3	3	3	4
10	0	0	0	0	0	0	0	0	0	0	3	3	3
11	0	0	0	0	0	0	0	0	0	0	0	3	3
12	0	0	0	0	0	0	0	0	0	0	0	0	3
13	0	0	0	0	0	0	0	0	0	0	0	0	0

Table 8 Characteristics of the instances used in numerical experiments.

Instance	$ \mathcal{T} $	The whole time period	The period during peaking hours	# Trains
H	60	6:30 - 7:30	6:35 - 7:30	6
I	75	6:30 - 7:45	7:00 - 7:45	14
J	90	6:30 - 8:00	7:00 - 8:00	18
K	100	6:50 - 8:30	7:00 - 8:30	24
L	120	6:30 - 8:30	7:00 - 8:30	33

example, GUROBI necessitates approximately 5,430 seconds to reach a near-optimal solution with a Gap of 5% for instance L. When employing TTCBD, however, a better solution is found within 2,300 seconds. We can also observe that including the strengthened optimality cuts worsens the solution efficiency. This can be explained by the fact that an integer model (35) has to be solved to generate these cuts, which introduces additional computational burden.

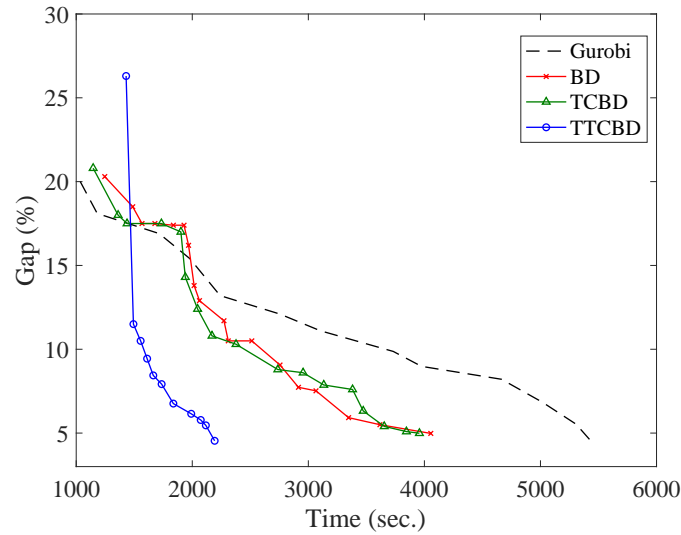
Table 9 Performance for GUROBI and the six variants of algorithms with a Gap limit of 5%

Instance index		GUROBI	BD	TCBD	TTCBD	TTSCBD	TRTCBD	TRTSCBD
H	Obj.	13,229.00	13,229.00	13,229.00	13,229.00	13,229.00	13,229.00	13,229.00
	Time (sec.)	1.48	4.07	3.84	4.42	6.24	9.43	15.05
I	Obj.	41,307.00	41,307.00	41,307.00	41,307.00	41,307.00	41,307.00	41,307.00
	Time (sec.)	56.37	168.78	139.08	124.31	399.64	223.68	1044.36
J	Obj.	43,042.00	43,128.00	43,098.00	43,042.00	43,463.00	43,042.00	43,080.00
	Time (sec.)	233.55	303.83	292.16	175.20	524.77	404.97	1316.53
K	Obj.	59,543.00	59,377.00	59,377.00	59,377.00	59,377.00	59,377.00	59,377.00
	Time (sec.)	910.43	2,185.19	22,39.00	895.33	1,240.36	1,678.77	3,491.24
L	Obj.	72,010.00	71,945.00	71,945.00	71,945.00	71,945.00	72,081.00	71,945.00
	Time (sec.)	5,428.54	4,176.90	4,006.74	2,192.77	5,859.72	7,524.54	15,800.98

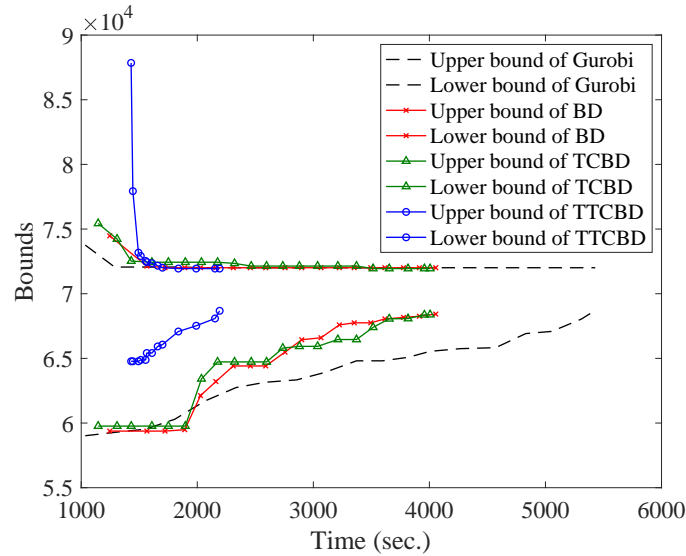
Figure 9 presents an overall comparison among GUROBI, BD, TCBD, and TTCBD in terms of the convergence trends of upper and lower bounds and the optimality gap over time with respect to the Instance L. Looking to Gap displayed in Figure 9(a), it is evident that TTCBD outperforms the other algorithms without the tree search strategy. Specifically, TTCBD finds a solution with a Gap of less than 5% within 2,200 seconds. In comparison, both TCBD and BD reach solutions with similar quality after 4,000 seconds, whereas GUROBI does not converge to a comparable solution within 5,000 seconds. Figure 9(b) provides detailed results of upper and lower bounds over time for these solution methods. Notably, the initial lower bound obtained by TTCBD is highest. The significant improvement in performance of TTCBD can be attributed to the incorporation of a tree search strategy, which facilitates strong branching and in-depth exploring for the lower bound. The second observation is that GUROBI, BD, and TCBD can quickly find a good upper bound, while the lower bound slowly increases. All in all, this experiment illustrates that TTCBD outperforms the other alternatives.

6.2.2. Benefits of integrating booking, directing and timetabling We next perform two experiments to assess the benefits of the integrated BDDT approach. In both experiments, we solve the instance with a study time horizon from 6:30 to 8:30, accommodating a departure time shift of up to 20 minutes. This setting is derived from the empirical results of the Beijing Metro Reservation Travel Pilot, wherein approximately 33% of commuters are willing to adjust their departure times by 5 to 15 minutes to utilize metro services. In the first experiment, weighting coefficients in the objective function are assigned equal values of 1, with both the booking and service ratios set at 20%. In the subsequent experiment, the weighting coefficients ω_t and ω_s are adjusted to 1 and 10 to emphasize the operator’s perspective, and the booking ratio is increased to 30%.

Based on these settings, we compare our BDDT approach against two alternative approaches.



(a) Gap



(b) Upper and lower bounds

Figure 9 Convergence trends of the upper and lower bounds and the Gap with respect to Instance L.

(i) *PFC*: Optimizing the passenger flow control strategy without allowing for trip shifting under the optimized train timetable through *BDDT*.

(ii) *SPE*: Simulating the evolution of passengers under the same optimized train timetable.

The optimized train timetables are visualized in Figure 10. Upon inputting the timetable with weighting coefficients into the *PFC* and *SPE* models, both models are proved to be infeasible. This result illustrates that, in the absence of trip shifting, the existing number of trains are incapable of satisfying all passenger demand while ensuring service fairness constraints. The results are in line with those of the previous experiment: encouraging passengers to shift their departure times would save the number of operated trains. Moreover, two additional trains are introduced, resulting in

the timetable shown in Figure 10(b). When applied to the PFC and SPE approaches, the results show that PFC is feasible while SPE remains infeasible. The reason is that the PFC method can control the number of boarding passengers at upstream stations, thus preserving capacity for those boarding at later stations. In essential, this finding highlights the necessity of implementing the passenger flow control strategy to optimize the allocation of capacity resources, thereby efficiently serving all passengers from a system-optimal perspective.

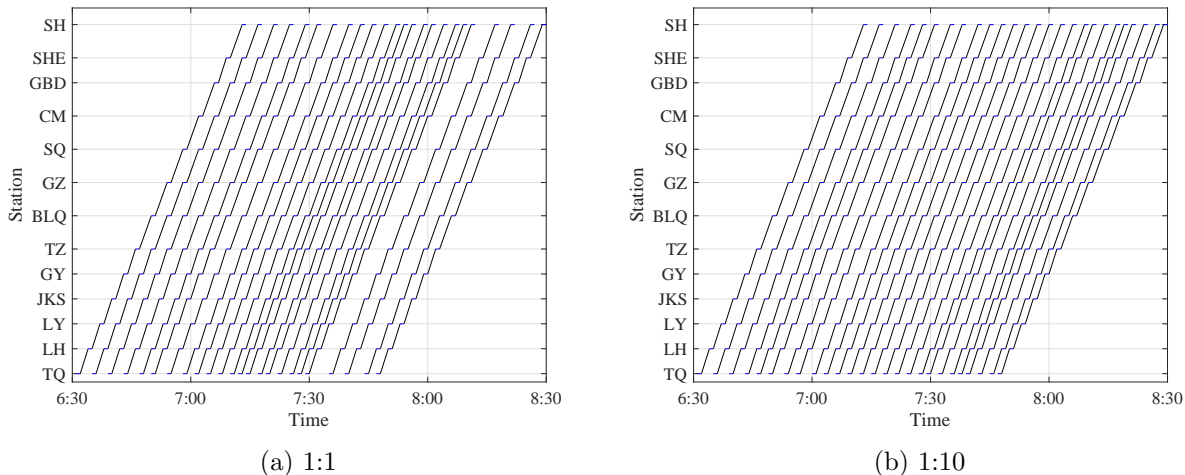


Figure 10 Optimized train timetables among different weighting coefficients.

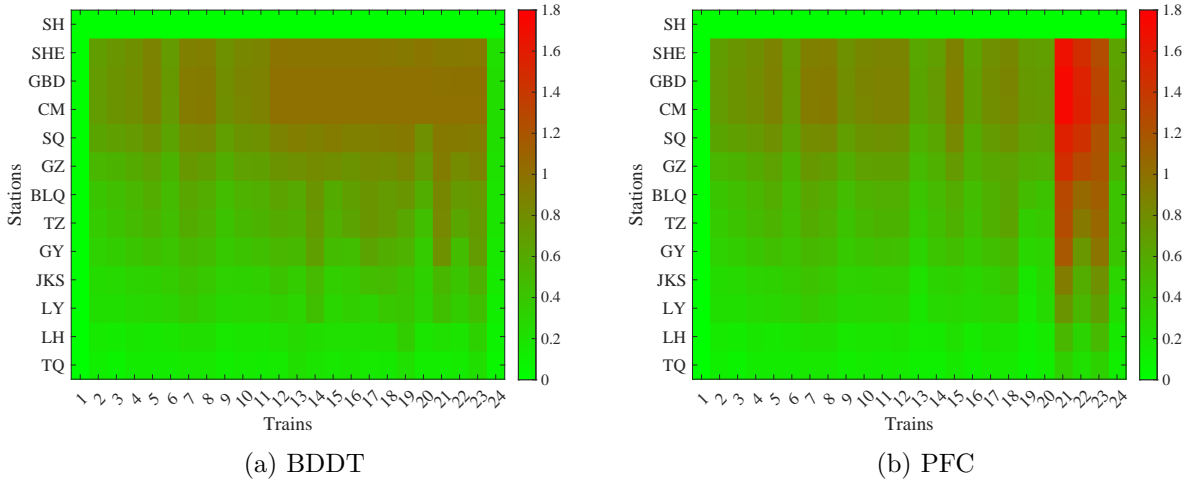
Further, to quantify the effectiveness of the proposed BDDT approach, we construct the other set of experiments. We relax the capacity constraints (24) in the PFC model, which is denoted as *relaxed PFC*. In Table 10, we present the results under the BDDT and relaxed PFC approaches, stating the waiting time of passengers, the additional government subsidies, and the number of overloading situations, the maximum number of in-vehicle passengers, and the relative differences of these indicators. The relative differences (denoted as Dev) is calculated using the formula $[(BDDT - PFC)/PFC] \times 100$ (%). The results show that encouraging passenger to shift their departure time leads to a reduction of 16.53% in the waiting time, complete mitigation of overloads by 100%, and 45.55% decrease in the maximum number of in-vehicle passengers. These findings emphasize the importance of implementing both the trip-shifting policy and the passenger flow control strategy at the same time, as opposed to only implementing the latter.

7. Conclusions

In this paper, we studied the integrated optimization of booking, directing and timetabling on oversaturated urban rail transit lines. Specifically, the main focus of this study consists of determining effective passenger directing approaches, which encompass passenger flow control and trip

Table 10 Performance comparison between the BDDT and relaxed PFC approaches.

Approach	Waiting time (min)	Lost revenue	Overloading (#)	Maximum number of in-vehicle passengers
PFC	97,152.00	0	21.00	3,481.00
BDDT	81,097.00	5,518.40	0	2,000.00
<i>Dev</i> (%)	-16.53	100.00	-100.00	45.55

**Figure 11** Comparison of utilized rates with respect to the capacity between the BDDT and relaxed PFC approaches.

shifting strategies, as well as to schedule train timetables. To this end, we developed an integrated INLP model to minimize the passengers' waiting time and the additional government subsidies. To improve the computational efficiency, we first linearized the above model by introducing auxiliary variables and big- M constraints, and derived the most appropriate values of big- M to obtain an ILP with a tighter upper bound. Thereafter, we proposed a Benders-decomposition-based approach in a branch-and-cut framework, which decomposes the integrated ILP model into a timetabling problem and a passenger assignment problem. To further enhance the solution efficiency, we proposed a novel decomposition method that incorporates partial passenger information into the timetabling problem to guide the optimization direction of the passenger assignment problem. We also integrated accelerated methods in terms of mathematical approaches and specific implementations.

To verify the effectiveness of the proposed approaches, two series of numerical experiments derived from a proof-of-concept line and the Beijing metro Batong line are implemented. The first series of experiments suggest that encouraging 21.14% of passengers to shift their arrival times by up to 10 minutes saves at least 8.33% of the number of operated trains. Compared to the minimum additional government subsidies to serve all passengers using the limited available trains, a 23.78% improvement in operational efficiency can be reached at the expense of a 1.00% increase in the additional government subsidies. The second experiment compares our integrated BDDT approach

and six variants of solution methods. The results indicate that the variant embedded with the cut loop, tailing off, and tree search strategies performs best in terms of execution time, especially for medium-scale and large-scale instances.

Our future research will focus on the following major aspects: (1) In this study, the time-dependent passenger demand is deterministic and pre-given. Future research could extend the model with uncertain passenger demand and forecasting algorithms to generate robust timetables. (2) Investigating how to integrate the reservation approach to multi-modal transportation systems to enhance the overall ecology of urban transportation networks is an interesting direction for future research.

Acknowledgments

This work was supported by the National Natural Science Foundation of China (Nos. 72288101, 72322022).

Appendix A: A framework for practical applications of the proposed approaches

In this section, we outline a framework for practical applications of our proposed integrated demand-side management and timetabling approach for an urban transit system.

Appendix B: Linearization of the proposed formulation

In this section, we provide a detailed description of the linearization of the proposed formulation (27).

Linearization of constraints (2). First, we introduce auxiliary variables q_{iut} for all $i \in \mathcal{I}, u \in \mathcal{S}, t \in \mathcal{T}$ to linearize constraints (2). Specifically, let $q_{iut} = x_{it} \sum_{v \in \mathcal{S}_{u+1}} r_{iuv}$, we have

$$\begin{cases} q_{iut} \leq M_u x_{it} \\ q_{iut} \leq \sum_{v \in \mathcal{S}_{u+1}} r_{iuv} \\ q_{iut} \geq \sum_{v \in \mathcal{S}_{u+1}} r_{iuv} - M_u (1 - x_{it}) \\ q_{iut} \in [0, M_u] \end{cases} \quad \forall i \in \mathcal{I}, u \in \mathcal{S}, t \in \mathcal{T}. \quad (46)$$

Therefore, the nonlinear constraints (2) are reformulated as the following linear version:

$$F^t = \sum_{i \in \mathcal{I}} \sum_{u \in \mathcal{S}} \sum_{t \in \mathcal{T}} (\hat{p}_{iut}^{wc} + p_{iut}^{wc}) + \sum_{i \in \mathcal{I}} \sum_{u \in \mathcal{S}} \sum_{t \in \mathcal{T}} q_{iut}. \quad (47)$$

Linearization of constraints (4). Besides, the linear version of constraints (4) which contain a nonlinear term of multiplication of a 0-1 variable with an integer variable is formulated as follows:

$$\begin{cases} p_{iut}^w \leq M_{ut} x_{it} \\ p_{iut}^w \leq \sum_{v \in \mathcal{S}_{u+1}} \sum_{t \leq t' \leq \min\{|\mathcal{T}|, t+i\}} \kappa_{uvtt'} \\ p_{iut}^w \geq \sum_{v \in \mathcal{S}_{u+1}} \sum_{t \leq t' \leq \min\{|\mathcal{T}|, t+i\}} \kappa_{uvtt'} - M_{ut} (1 - x_{it}) \\ p_{iut}^w \in [0, M_{ut}] \end{cases} \quad \forall i \in \mathcal{I}, u \in \mathcal{S}, t \in \mathcal{T}. \quad (48)$$

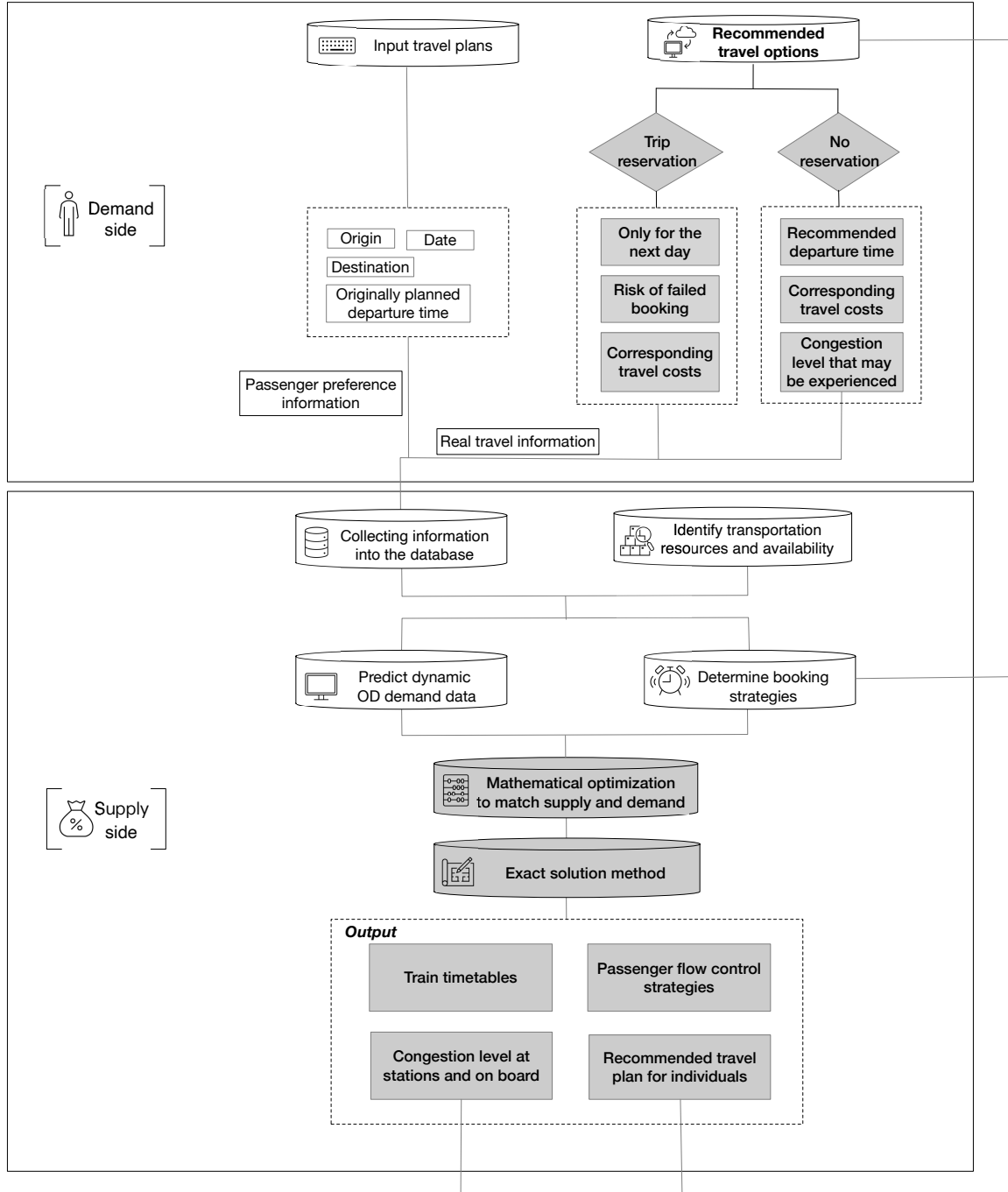


Figure 12 A framework for practical applications.

Linearization of constraints (6) and (7). To derive equivalent linear forms of constraints (6) and (7), we first introduce auxiliary variables $\theta_{itt'}, \forall i \in \mathcal{I}, t \in \mathcal{T}, t' \leq t$. Let $\theta_{itt'} = x_{it}x_{it'}$, we have

$$\begin{cases} \theta_{itt'} \leq x_{it} \\ \theta_{itt'} \leq x_{it'} \\ \theta_{itt'} \geq x_{it} + x_{it'} - 1 \\ \theta_{itt'} \in [0, 1], \end{cases} \quad \forall i \in \mathcal{I}, t, t' \in \mathcal{T}, t' \leq t. \quad (49)$$

The linear version of constraints (6) can be expressed as

$$\hat{p}_{iut}^{wc} = \sum_{t' \in \mathcal{T}, t' \leq t} \sum_{v \in \mathcal{S}_{u+1}} \theta_{itt'} \hat{D}_{uvt'} \quad \forall i \in \mathcal{I}, u \in \mathcal{S}, t \in \mathcal{T}. \quad (50)$$

Further, by introducing auxiliary variables $\mu_{iutt'}, \forall i \in \mathcal{I}, u \in \mathcal{S}, t \in \mathcal{T}, t' \leq t$, let $\mu_{iutt'} = \theta_{itt'} \sum_{v \in \mathcal{S}_{u+1}} \sum_{t' \leq t'' \leq \min\{|\mathcal{T}|, t' + \iota\}} \kappa_{uvt't''}$, we have

$$\begin{cases} \mu_{iutt'} \leq M_{ut'} \theta_{itt'} \\ \mu_{iutt'} \leq \sum_{v \in \mathcal{S}_{u+1}} \sum_{t' \leq t'' \leq \min\{|\mathcal{T}|, t' + \iota\}} \kappa_{uvt't''} \\ \mu_{iutt'} \geq \sum_{v \in \mathcal{S}_{u+1}} \sum_{t' \leq t'' \leq \min\{|\mathcal{T}|, t' + \iota\}} \kappa_{uvt't''} - M_{ut'} (1 - \theta_{itt'}) \\ \mu_{iutt'} \in [0, M_{ut'}] \end{cases} \quad \forall i \in \mathcal{I}, u \in \mathcal{S}, t \in \mathcal{T}, t' \leq t. \quad (51)$$

The linear form of constraints (7) can be expressed as

$$p_{iut}^{wc} = \sum_{v \in \mathcal{S}_{u+1}} \sum_{t' \in \mathcal{T}, t' \leq t} \sum_{t'' \leq t' \leq \min\{|\mathcal{T}|, t' + \iota\}} \mu_{iuvtt't''} \quad \forall i \in \mathcal{I}, u \in \mathcal{S}, t \in \mathcal{T}. \quad (52)$$

Linearization of constraints (18). We define auxiliary variables $\Gamma_{iuvt'}$, let $w_{iuvt'} = z_{it'} \sum_{t' \leq t \leq \min\{|\mathcal{T}|, t' + \iota\}} \kappa_{uvt't}$ for all $i \in \mathcal{I}, u \in \mathcal{S}, v \in \mathcal{S}_{u+1}, t' \in \mathcal{T}$, the linearization results of this term in constraint (18) are shown below:

$$\begin{cases} \Gamma_{iuvt'} \leq M_{uvt'} z_{it'} \\ \Gamma_{iuvt'} \leq \sum_{t' \leq t \leq \min\{|\mathcal{T}|, t' + \iota\}} \kappa_{uvt't} \\ \Gamma_{iuvt'} \geq \sum_{t' \leq t \leq \min\{|\mathcal{T}|, t' + \iota\}} \kappa_{uvt't} - M_{uvt'} (1 - z_{it'}) \\ \Gamma_{iuvt'} \in [0, M_{uvt'}] \end{cases} \quad \forall i \in \mathcal{I}, u \in \mathcal{S}, v \in \mathcal{S}_{u+1}, t' \in \mathcal{T}. \quad (53)$$

Thus, we have

$$w_{iuv} = \begin{cases} \sum_{t' \in \mathcal{T}} \Gamma_{iuvt'} & \text{if } i = 1 \\ \sum_{t' \in \mathcal{T}} \Gamma_{iuvt'} - \sum_{j=1}^{i-1} b_{juv} & \text{if } i \in \mathcal{I} \setminus \{1\} \end{cases} \quad \forall u \in \mathcal{S}, v \in \mathcal{S}_{u+1}. \quad (54)$$

Appendix C: Model extensions adopting off-peak and peak pricing policy and elastic passenger demand from other transportation modes

In this section, we formulate two extended models that incorporate off-peak and peak pricing policy and elastic passenger demand from other transportation modes into consideration.

(a) Extension with the off-peak and peak pricing policy. In reality, some rail transit systems, such as the metro in Washington DC and London, employ the time-varying pricing policy, known as *Off-Peak and Peak Pricing*. This approach incentivizes passengers to travel during less congested periods, while charging higher fares during peak hours. Our formulation (27) can be extended to incorporate this pricing policy, as detailed below:

$$\begin{aligned} \min \quad & F^t & (55a) \\ \text{s.t.} \quad & \sum_{u \in \mathcal{S}} \sum_{v \in \mathcal{S}_{u+1}} \sum_{t \in \mathcal{T}} \nu_{uvt} \left(\sum_{t' \leq t \leq \min\{|\mathcal{T}|, t' + \iota\}} \kappa_{uvtt'} + \hat{D}_{uvt} \right) \geq \end{aligned}$$

$$\varkappa \sum_{u \in \mathcal{S}} \sum_{v \in \mathcal{S}_{u+1}} \sum_{t \in \mathcal{T}} \varepsilon_{uv} (D_{uvt} + \hat{D}_{uvt}), \quad (55b)$$

$$(2), (4) - (7), (8) - (26),$$

where ν_{uvt} is the ticket fare at timestamp t for OD from stations u to v under the off-peak and peak pricing policy, and $\varkappa \in [0, 100]$ (unit: %) represents the percentage of operator's revenue under the off-peak and peak pricing policy versus the revenue under static ticket fares. Here, the objective function (55a) aims to minimize the total waiting time of passengers. Constraints (55b) are formulated to ensure that the operator's fare revenue is not less than \varkappa times the original revenue with the static ticket price.

(b) Extension with the elastic passenger demand from other transportation modes. Considering the entire urban transportation system, which includes various modes, the off-peak and peak pricing policy in the URT network, which provides lower fares during off-peak periods, has the potential to enhance the attractiveness and cost-effectiveness of the URT. Specifically, this policy could encourage passengers who typically use alternative transportation modes to shift to the URT system during low-peak hours.

To formulate this extended problem, we introduce a parameter ϵ_t to represent the scaling coefficient at timestamp t . A decision variable Λ_{uvt} is defined to denote the ticket fare at timestamp t for OD from stations u to v under the off-peak and peak pricing policy. Furthermore, we formulate the number of elastic passengers from other transportation modes who head to station $v \in \mathcal{S}_{u+1}$ and shift to take the URT at station $u \in \mathcal{S}$ and time $t \in \mathcal{T}$ as:

$$\epsilon_t \frac{\max_{t'' \in \mathcal{T}} \{\Lambda_{uvt''}\} - \Lambda_{uvt}}{\Lambda_{uvt}} D_{uvt}.$$

When $\Lambda_{uvt} = \max_{t'' \in \mathcal{T}} \{\Lambda_{uvt''}\}$, indicating the ticket price at timestamp t for OD from stations u to v is the highest value during the study time horizon, lacks additional appeal. Conversely, the attractiveness coefficient for passengers of other modes is given by $\epsilon_t \frac{\max_{t'' \in \mathcal{T}} \{\Lambda_{uvt''}\} - \Lambda_{uvt}}{\Lambda_{uvt}}$.

Based on the above definitions, we can now formulate this problem as follows:

$$\begin{aligned} \min \quad & F^t \\ \text{s.t.} \quad & \sum_{\max\{0, t-i\} \leq t' \leq t} \kappa_{uvtt'} = D_{uvt} + \epsilon_t \frac{\max_{t'' \in \mathcal{T}} \{\Lambda_{uvt''}\} - \Lambda_{uvt}}{\Lambda_{uvt}} D_{uvt} \quad \forall u \in \mathcal{S}, v \in \mathcal{S}_{u+1}, t \in \hat{\mathcal{T}}, \end{aligned} \quad (56a)$$

$$\kappa_{uvtt'} = \begin{cases} D_{uvt} + \epsilon_t \frac{\max_{t'' \in \mathcal{T}} \{\Lambda_{uvt''}\} - \Lambda_{uvt}}{\Lambda_{uvt}} D_{uvt} & \text{if } t' = t \\ 0 & \text{otherwise} \end{cases} \quad \forall u \in \mathcal{S}, v \in \mathcal{S}_{u+1}, t \in \mathcal{T} \setminus \hat{\mathcal{T}}, \quad (56b)$$

$$\sum_{i \in \mathcal{I}} b_{iuv} = \sum_{t \in \mathcal{T}} D_{uvt} + \epsilon_t \frac{\max_{t'' \in \mathcal{T}} \{\Lambda_{uvt''}\} - \Lambda_{uvt}}{\Lambda_{uvt}} D_{uvt} \quad \forall u \in \mathcal{S}, v \in \mathcal{S}_{u+1}, \quad (56c)$$

$$\begin{aligned} \sum_{u \in \mathcal{S}} \sum_{v \in \mathcal{S}_{u+1}} \sum_{t \in \mathcal{T}} \Lambda_{uvt} \left(\sum_{t \leq t' \leq \min\{|\mathcal{T}|, t+i\}} \kappa_{uvtt'} + \hat{D}_{uvt} \right) \\ \geq \varkappa \sum_{u \in \mathcal{S}} \sum_{v \in \mathcal{S}_{u+1}} \sum_{t \in \mathcal{T}} \varepsilon_{uv} (D_{uvt} + \hat{D}_{uvt}), \end{aligned} \quad (56d)$$

$$\Lambda_{uvt} \in \mathbb{R}_+ \quad \forall u \in \mathcal{S}, v \in \mathcal{S}_{u+1}, t \in \mathcal{T}, \quad (56e)$$

$$(2), (4) - (7), (8) - (13), (16) - (26).$$

The objective function aims to minimize the total waiting time of passengers. Similar to constraints (14) and (15), constraints (56a) and (56b) are formulated to calculate the number of arrival passengers at each timestamp and station after passengers shifting their departure times. Constraints (56c) ensure that the already loyal to the metro or newly attracted passengers are all served. Constraints (56d) guarantee that the operator's revenue under the off-peak and peak pricing policy is not less than \varkappa times the original revenue with the static passenger demand and the ticket price. Lastly, constraints (56e) give the domain of the decision variable Λ_{uvt} .

References

- Bao, Y., Yang, H., Gao, Z., Xu, H., 2023. How do pre-event activities alleviate congestion and increase attendees' travel utility and the venue's profit during a special event? *Transportation Research Part B: Methodological* 173, 332–353.
- Barz, C., Gartner, D., 2016. Air cargo network revenue management. *Transportation Science* 50, 1206–1222.
- Benders, J., 1962. Partitioning procedures for solving mixed-variables programming problems. *Numerische Mathematik* 4, 238–252.
- Binder, S., Maknoon, M., Sharif Azadeh, S., Bierlaire, M., 2021. Passenger-centric timetable rescheduling: A user equilibrium approach. *Transportation Research Part C: Emerging Technologies* 132, 103368.
- China News, 2020. The trial of station entry reservation will be launched at Caofang Station of Beijing Subway Line 6 starting from April 29th. <https://m.chinanews.com/wap/detail/chs/zw/9169668.shtml>. [Accessed April 12, 2024].
- Copeland, D.G., McKenney, J.L., 1988. Airline reservations systems: Lessons from history. *MIS Quarterly* 12, 353–370.
- Croella, A.L., Luteberget, B., Mannino, C., Ventura, P., 2024. A maxsat approach for solving a new dynamic discretization discovery model for train rescheduling problems. *Computers & Operations Research* 167, 106679.
- Di, Z., Yang, L., Shi, J., Zhou, H., Yang, K., Gao, Z., 2022. Joint optimization of carriage arrangement and flow control in a metro-based underground logistics system. *Transportation Research Part B: Methodological* 159, 1–23.
- Ding, H., Yang, H., Qin, X., Xu, H., 2023. Credit charge-cum-reward scheme for green multi-modal mobility. *Transportation Research Part B: Methodological* 178, 102852.
- Fischetti, M., Ljubić, I., Sinnl, M., 2016. Benders decomposition without separability: A computational study for capacitated facility location problems. *European Journal of Operational Research* 253, 557–569.
- Fischetti, M., Ljubić, I., Sinnl, M., 2017. Redesigning Benders decomposition for large-scale facility location. *Management Science* 63, 2146–2162.
- He, X., Chen, X.M., Xiong, C., Zhu, Z., Zhang, L., 2017. Optimal time-varying pricing for toll roads under multiple objectives: A simulation-based optimization approach. *Transportation Science* 51, 412–426.
- Hu, Y., Li, S., Wang, Y., Zhang, H., Wei, Y., Yang, L., 2023. Robust metro train scheduling integrated with skip-stop pattern and passenger flow control strategy under uncertain passenger demands. *Computers & Operations Research* 151, 106116.
- Leutwiler, F., Corman, F., 2022. A logic-based benders decomposition for microscopic railway timetable planning. *European Journal of Operational Research* 303, 525–540.
- Leutwiler, F., Corman, F., 2023. Set covering heuristics in a benders decomposition for railway timetabling. *Computers & Operations Research* 159, 106339.
- Li, S., Dessouky, M.M., Yang, L., Gao, Z., 2017. Joint optimal train regulation and passenger flow control strategy for high-frequency metro lines. *Transportation Research Part B: Methodological* 99, 113–137.
- Li, X., Yang, H., Ke, J., 2023. Booking cum rationing strategy for equitable travel demand management in road networks. *Transportation Research Part B: Methodological* 167, 261–274.
- Liang, J., Lyu, G., Teo, C.P., Gao, Z., 2023. Online passenger flow control in metro lines. *Operations Research* 71, 768–775.
- Liu, R., Li, S., Yang, L., 2020. Collaborative optimization for metro train scheduling and train connections combined with passenger flow control strategy. *Omega* 90, 101990.
- Liu, W., Yang, H., Yin, Y., 2015. Efficiency of a highway use reservation system for morning commute. *Transportation Research Part C: Emerging Technologies* 56, 293–308.
- Lu, Y., Yang, L., Yang, H., Zhou, H., Gao, Z., 2023. Robust collaborative passenger flow control on a congested metro line: A joint optimization with train timetabling. *Transportation Research Part B: Methodological* 168, 27–55.
- Lu, Y., Yang, L., Yang, K., Gao, Z., Zhou, H., Meng, F., Qi, J., 2022. A distributionally robust optimization method for passenger flow control strategy and train scheduling on an urban rail transit line. *Engineering* 12, 202–220.
- Meng, F., Yang, L., Shi, J., Jiang, Z., Gao, Z., 2022. Collaborative passenger flow control for oversaturated metro lines: A stochastic optimization method. *Transportmetrica A: Transport Science* 18, 619–658.
- Ministry of Transport of the People's Republic of China, 2022. The transportation authority optimizes the capacity to serve the large passenger flow, so that the city artery keeps surging up. https://www.mot.gov.cn/jiaotongyaowen/202212/t20221228_3730584.html/. [Accessed March 29, 2023].
- Motoring, 2024. Electronic Road Pricing. <https://onemotoring.lta.gov.sg/content/onemotoring/home/driving/ERP.html>. [Accessed April 12, 2024].
- Nederlandse Spoorwegen, 2024. When can you travel with a discount? <https://www.ns.nl/en/featured/traveling-with-discount/when-can-you-travel-with-a-discount.html>. [Accessed April 12, 2024].
- People, 2020. Reservations can reduce waiting in line due to passenger flow control. <http://bj.people.com.cn/n2/2020/0430/c82840-33987970.html>. [Accessed September 12, 2024].
- Polinder, G.J., Cacchiani, V., Schmidt, M., Huisman, D., 2022. An iterative heuristic for passenger-centric train timetabling with integrated adaption times. *Computers & Operations Research* 142, 105740.

- Rahmaniani, R., Ahmed, S., Crainic, T.G., Gendreau, M., Rei, W., 2020. The Benders dual decomposition method. *Operations Research* 68, 878–895.
- Robenek, T., Sharif Azadeh, S., Maknoon, Y., De Lapparent, M., Bierlaire, M., 2018. Train timetable design under elastic passenger demand. *Transportation Research Part B: Methodological* 111, 19–38.
- Rothstein, M., 1985. OR and the airline overbooking problem. *Operations Research* 33, 237–248.
- Shi, J., Yang, L., Yang, J., Gao, Z., 2018. Service-oriented train timetabling with collaborative passenger flow control on an oversaturated metro line: An integer linear optimization approach. *Transportation Research Part B: Methodological* 110, 26–59.
- Transport for London, 2024. Congestion Charge zone. <https://tfl.gov.uk/modes/driving/congestion-charge/congestion-charge-zone>. [Accessed April 12, 2024].
- United Nations, 2019. Shifting Demographics: A Visual Guide. <https://www.un.org/en/un75/shifting-demographics>. [Accessed March 28, 2023].
- Van Lieshout, R.N., Dalmeijer, K., 2024. A unified approach to evaluation and routing in public transport systems. [arXiv:2207.09969](https://arxiv.org/abs/2207.09969).
- Wang, L., Jin, J.G., Sibul, G., Wei, Y., 2023. Designing metro network expansion: Deterministic and robust optimization models. *Networks and Spatial Economics* 23, 317–347.
- Xia, D., Ma, J., Sharif Azadeh, S., 2024. Integrated timetabling and vehicle scheduling of an intermodal urban transit network: A distributionally robust optimization approach. *Transportation Research Part C: Emerging Technologies* 162, 104610.
- Xia, D., Ma, J., Sharif Azadeh, S., Zhang, W., 2023. Data-driven distributionally robust timetabling and dynamic-capacity allocation for automated bus systems with modular vehicles. *Transportation Research Part C: Emerging Technologies* 155, 104314.
- Xiao, L.L., Huang, H.J., Liu, R., 2015. Congestion behavior and tolls in a bottleneck model with stochastic capacity. *Transportation Science* 49, 46–65.
- Yang, H., Bell, M.G.H., 1998. Models and algorithms for road network design: A review and some new developments. *Transport Reviews* 18, 257–278.
- Yang, H., Shao, C., Wang, H., Ye, J., 2020. Integrated reward scheme and surge pricing in a ridesourcing market. *Transportation Research Part B: Methodological* 134, 126–142.
- Yang, H., Wang, X., 2011. Managing network mobility with tradable credits. *Transportation Research Part B: Methodological* 45, 580–594.
- Yin, J., D’Ariano, A., Wang, Y., Yang, L., Tang, T., 2021. Timetable coordination in a rail transit network with time-dependent passenger demand. *European Journal of Operational Research* 295, 183–202.
- Yin, J., Pu, F., Yang, L., D’Ariano, A., Wang, Z., 2023. Integrated optimization of rolling stock allocation and train timetables for urban rail transit networks: A Benders decomposition approach. *Transportation Research Part B: Methodological* 176, 102815.
- Yuan, Y., Li, S., Liu, R., Yang, L., Gao, Z., 2023. Decomposition and approximate dynamic programming approach to optimization of train timetable and skip-stop plan for metro networks. *Transportation Research Part C: Emerging Technologies* 157, 104393.